Annals of Physics 348 (2014) 228–255

Contents lists available at ScienceDirect

Annals of Physics

journal homepage: www.elsevier.com/locate/aop

# Generalized Beth–Uhlenbeck approach to mesons and diquarks in hot, dense quark matter

D. Blaschke [a,b,*], M. Buballa [c], A. Dubinin [a], G. Röpke [d], D. Zablocki [a,c]

[a] *Institute for Theoretical Physics, University of Wrocław, pl. M. Borna 9, 50-204 Wrocław, Poland*

[b] *Laboratory for Theoretical Physics, Joint Institute for Nuclear Research, Joliot-Curie ul. 6, 141980 Dubna, Russia*

[c] *Theoriezentrum, Institut für Kernphysik, Technische Universität Darmstadt, Schlossgartenstr. 2, 64289 Darmstadt, Germany*

[d] *Institut für Physik, Universität Rostock, Universitätsplatz 3, 18055 Rostock, Germany*

ARTICLE INFO

*Article history:*
Received 6 January 2014
Accepted 1 June 2014
Available online 9 June 2014

*Keywords:*
Quark–gluon plasma
Meson
Diquark
Bethe–Salpeter equation
Beth–Uhlenbeck equation
Mott effect

ABSTRACT

An important first step in the program of hadronization of chiral quark models is the bosonization in meson and diquark channels. This procedure is presented at finite temperatures and chemical potentials for the SU(2) flavor case of the NJL model with special emphasis on the mixing between scalar meson and scalar diquark modes which occurs in the 2SC color superconducting phase. The thermodynamic potential is obtained in the Gaussian approximation for the meson and diquark fields and it is given in the Beth–Uhlenbeck form. This allows a detailed discussion of bound state dissociation in hot, dense matter (Mott effect) in terms of the in-medium scattering phase shift of two-particle correlations. It is shown for the case without meson–diquark mixing that the phase shift can be separated into a continuum and a resonance part. In the latter, the Mott transition manifests itself by a change of the phase shift at threshold by $\pi$ in accordance with Levinson's theorem, when a bound state transforms to a resonance in the scattering continuum. The consequences for the contribution of pionic correlations to the pressure are discussed by evaluating the Beth–Uhlenbeck equation of state in different approximations. A

* Corresponding author at: Institute for Theoretical Physics, University of Wrocław, pl. M. Borna 9, 50-204 Wrocław, Poland.
*E-mail addresses:* blaschke@ift.uni.wroc.pl, david.blaschke@gmail.com (D. Blaschke), michael.buballa@physik.tu-darmstadt.de (M. Buballa), aleksandr.dubinin@ift.uni.wroc.pl (A. Dubinin), gerd.roepke@uni-rostock.de (G. Röpke), zablocki@ift.uni.wroc.pl (D. Zablocki).

http://dx.doi.org/10.1016/j.aop.2014.06.002

similar discussion is performed for the scalar diquark channel in the normal phase. Further developments and applications of the developed approach are outlined.



## 1. Introduction

One of the long-standing problems of low-energy hadron physics concerns the hadronization of QCD, i.e., the transformation of QCD formulated as a gauge theory of quark and gluon fields to an effective theory formulated in terms of hadrons, the observable low-energy degrees of freedom. The general idea is to start from the path integral representation of the partition function (generating functional) of QCD and to "integrate out" the elementary quark and gluon degrees of freedom, leaving an effective theory in terms of collective hadronic degrees of freedom. This task may be schematically depicted as the map

$$\mathscr{Z}_{\rm QCD} = \int \mathscr{D}\bar{q}\mathscr{D}q\mathscr{D}A \exp\{\mathscr{A}_{\rm QCD}[\bar{q}, q, A]\} \longrightarrow \int \mathscr{D}M\mathscr{D}\bar{B}\mathscr{D}B \exp\{\mathscr{A}_{\rm eff}[\bar{B}, B, M]\}, \tag{1}$$

where $\mathscr{A}_{\rm QCD}[\bar{q}, q, A]$ is the Euclidean action functional of QCD in terms of quark $(\bar{q}, q)$ and gluon $(A)$ fields, while $\mathscr{A}_{\rm eff}[\bar{B}, B, M]$ is an effective low-energy action functional in terms of baryon $(\bar{B}, B)$ and meson $(M)$ fields. Since the map (1) involves, among others, the still open problem of quark confinement, we do not aim at a solution on the level of mathematical rigor. A slightly modified, solvable version of this program (1) does start from the global color model of QCD where all nonabelian aspects of the gluon sector are absorbed into nonperturbative gluon $n$-point functions (Schwinger functions) starting with the gluon propagator (2-point function) coupling to quark currents via nonperturbative vertex functions (3-point functions), see [1–4] for basic reviews.

After Fierz rearrangement of the current–current interaction [5,6], the theory obtains the Yukawa-like form with Dirac quark fields coupled to the spectrum of meson and diquark channels, thus generating 4-fermion interactions in the relevant quark–antiquark and quark–quark bilinears [7,8], see also [9].

The hadronization proceeds further via the two-step Hubbard–Stratonovich procedure by: (1) introducing auxiliary collective fields and functional integration over them such that the 4-fermion interaction terms are replaced by Yukawa couplings to the collective fields, and (2) integrating out the quark fields so that an effective theory results which is formulated in meson and diquark degrees of freedom, highly nonlinear due to the Fermion determinant, recognizable as "Tr ln" terms in the effective bosonized action.

In this way one obtains a bosonized chiral quark model, but not yet the desired hadronization in terms of mesons and baryons, the physical degrees of freedom of low-energy QCD and hadronic matter. A possible scheme for introducing baryons as quark–diquark bound states and integrating out the colored and therefore not asymptotically observable diquark fields has been suggested by Cahill and collaborators [7,10–12]. It was afterwards elaborated by Reinhardt [8] and developed further by including the solitonic aspects of a field theoretic description of the nucleon [13], see also Refs. [14,9, 15,16]. Introductory reviews on the latter can be found, *e.g.,* in [17–19].

It is the aim of our study to extend the hadronization of effective chiral quark models for QCD to nonzero temperatures and densities. The goal is to investigate the modification of thermodynamic properties of hadronic matter evoked under extreme conditions by the onset of (partial) chiral symmetry restoration. In this first part of our work we investigate in detail the two-particle correlations (mesons and diquarks) in a hot and dense quark matter medium and the response of their spectral properties to medium dependent mean fields signaling chiral symmetry breaking (quark mass gap) and color superconductivity (diquark pairing gap). Of central interest is the relation of the meson and diquark spectrum to the density and temperature dependence of these order parameters (quark mass and pairing gap), the question under which conditions mesons and diquarks may exist as real bound

states or appear only as a correlation in the continuum of quark–antiquark and quark–quark scattering states, resp. The transition of a correlation from the discrete bound state spectrum to a resonant continuum state is called Mott effect and will be a central theme for our study. When it occurs at low temperatures and high densities under fulfillment of the conditions for Bose condensation, the Mott effect serves as a mechanism for the BEC–BCS crossover [20] which recently became very topical when in atomic traps this transition could be studied in detail under laboratory conditions.

While numerous works have recently studied the thermodynamics of quark matter on the mean-field level including the effects of the medium dependence of the order parameters, not so much is known beyond the mean field, about hadronic correlations and their backreaction to the structure of the model QCD phase diagram and its thermodynamics. Here we will elaborate on the generalized Beth–Uhlenbeck form of the equation of state (EoS) which is systematically extended from studying mesonic correlations [21] to the inclusion of diquark degrees of freedom. To that end we will employ a Nambu–Jona-Lasinio-type quark model with four-point interactions in mesonic (quark–antiquark) and diquark (quark–quark) channels. We shall discuss here the importance of the interplay of the resonant states with the residual non-resonant in the continuum of scattering states. Due to the Levinson theorem both contributions have the tendency to compensate each other in quark matter above the Mott transition [22–24], see also [25].

The most intriguing questions will occur when on the basis of this in-medium bosonized effective chiral quark model the next step of the hadronization program nucleon will be performed and diquarks will be "integrated out" in favor of baryons so that nuclear matter can be described in the model QCD phase diagram. Exploratory studies within the framework of an effective local NJL-type model for the quark–diquark interaction vertex have revealed a first glimpse at the modification of the nucleon spectral function in the different regions of the model QCD phase diagram, including chirally restored and color superconducting phases [26].

We will prepare the ground for a Beth–Uhlenbeck description of nuclear matter, to be discussed in future work. In particular, at zero temperature the structure of a Walecka model for nuclear matter shall emerge under specified conditions. Earlier work in this direction [27–29] has demonstrated this possibility although no unified description of the nuclear-to-quark matter transition has been possible and the elucidation of physical mechanisms for the very transition between the hadronic and the quark matter phases of low energy QCD has been spared out. Our study aims at indicating directions for filling this gap by providing a detailed discussion of the Mott mechanism for the dissociation of hadronic bound states of quarks within the NJL model description of low-energy QCD on the example of two-particle correlations (mesons and diquarks).

Our approach can be considered as complementary to lattice gauge theory, where $\mathscr{Z}_{\rm QCD}$ is calculated in ab initio Monte-Carlo simulations without further approximations other than the discretization of space–time [30,31]. While being more rigorous, lattice calculations are often lacking a clear physical interpretation of the results. Moreover, because of the fermion sign problem, they are restricted to vanishing or small chemical potential. In this situation, effective chiral quark model approaches, like the one employed here, can give invaluable methodological guidance to elucidate how effects like bound state dissociation in hot and dense quark matter, as seen in spectral functions, may manifest themselves in two-particle correlators which are objects accessible to lattice QCD simulations.

This work is organized as follows. In Section 2 we define our model and derive the thermodynamic potential in mean-field approximation and its corrections to Gaussian order in normal and color superconducting matter. The corresponding meson and diquark spectra are discussed in Section 3. Section 4 is the main part of this article. Here we derive a generalized Beth–Uhlenbeck form for the thermodynamic potential of two-particle correlations in quark matter as the appropriate representation for discussing the Mott effect, the dissociation of hadronic bound states of quarks induced by the lowering of the quark continuum by the chiral symmetry restoration at finite temperatures and chemical potentials. We evaluate the temperature dependence of the phase shifts for pion, sigma meson and scalar diquark interaction channels and obtain the corresponding correlation contributions to the EoS. In Section 4 we give an outlook to further developments and applications of the formalism. In Section 5 we summarize our main results and present the conclusions of this work.

## 2. The model: mean field approximation and beyond

We consider a system of quarks with $N_f = 2$ flavor and $N_c = 3$ color degrees of freedom at temperature $T$ and chemical potential $\mu$, described by the Nambu–Jona-Lasinio (NJL) type Lagrangian

$$\mathscr{L} = \mathscr{L}_0 + \mathscr{L}_{\rm S} + \mathscr{L}_{\rm V} + \mathscr{L}_{\rm D}. \tag{2}$$

The free part is given by

$$\mathscr{L}_0 = \bar{q}(\mathrm{i}\partial\!\!\!/ - m_0 + \mu\gamma_0)q, \tag{3}$$

with the bare quark mass $m_0$. Here we have assumed isospin symmetry, *i.e.,* equal masses and chemical potentials for up and down quarks. The quarks interact via local four-point vertices in the scalar–isoscalar, pseudoscalar–isovector and vector–isoscalar quark–antiquark channels,

$$\mathscr{L}_{\rm S} = G_{\rm S}\left[(\bar{q}q)^2 + (\bar{q}\mathrm{i}\gamma_5\vec{\tau}q)^2\right], \tag{4}$$

$$\mathscr{L}_{\rm V} = -G_{\rm V}(\bar{q}\gamma_\mu q)^2, \tag{5}$$

augmented with a quark–quark interaction in the scalar color-antitriplet channel,

$$\mathscr{L}_{\rm D} = G_{\rm D}\sum_{A=2,5,7}(\bar{q}\mathrm{i}\gamma_5\tau_2\lambda_A q^c)(\bar{q}^c\mathrm{i}\gamma_5\tau_2\lambda_A q). \tag{6}$$

Here $q^c = C\bar{q}^T$ with $C = \mathrm{i}\gamma^2\gamma^0$ denote the charge conjugate quark fields, $\lambda_A$, $A = 2, 5, 7$, the anti-symmetric Gell-Mann matrices in color space and $\tau_i$, $i = 1, 2, 3$, the Pauli matrices in flavor space. $G_{\rm S}$, $G_{\rm V}$ and $G_{\rm D}$ are dimensionful coupling constants.

Eventually, one should also couple the quarks to an effective Polyakov loop variable [32–34], in order to describe confinement effects in a more realistic way. Although in principle straightforward, this would lead to the appearance of more complicated dispersion relations in the expressions below [35]. For simplicity, we therefore leave this extension for a later publication.

Our model then has five parameters: the bare quark mass $m_0$, the coupling constants $G_{\rm S}$, $G_{\rm V}$ and $G_{\rm D}$ and a cutoff parameter $\Lambda$, which is needed because the interaction is not renormalizable. While $m_0$, $G_{\rm S}$ and $\Lambda$ are typically fitted to vacuum properties (mass and decay constant) of the pion and to the chiral condensate [36–38], the two other coupling constants are less constrained. They are sometimes related to the scalar coupling via Fierz transformation of a color-current interaction, which yields $G_{\rm V} = G_{\rm S}/2$ and $G_{\rm D} = 3/4G_{\rm S}$. Alternatively, $G_{\rm V}$ can be fixed by fitting the mass of vector mesons, which gives higher values [39]. Another possibility is to constrain $G_{\rm V}$ and $G_{\rm D}$ from compact star and heavy-ion phenomenology [40]. In the present paper, we will specify the parameters only in the context of the numerical examples discussed in Section 4, while most of the analytic expressions are more general. In future extensions of the model one could then try to fix $G_{\rm V}$ and $G_{\rm D}$ by fitting baryon and nuclear matter properties.

The bulk thermodynamic properties of the model at temperature $T$ and chemical potential $\mu$ are encoded in the thermodynamic potential per volume

$$\Omega(T,\mu) = -\frac{T}{V}\ln\mathscr{Z}(T,\mu), \tag{7}$$

with the grand partition function $\mathscr{Z}$ which is given as a functional integral involving the above Lagrangian,

$$\mathcal{Z} = \int\mathscr{D}q\mathscr{D}\bar{q}\exp\left[\int\mathrm{d}^4x_E\ \mathscr{L}\right], \tag{8}$$

where $\int\mathrm{d}^4x_E = \int_0^\beta\mathrm{d}\tau\int\mathrm{d}^3\mathbf{x}$ denotes an integration over the Euclidean four-volume, *i.e.,* over the three-space with volume $V$ and imaginary time $\tau$ restricted to the interval between 0 and $\beta = 1/T$. We perform a bosonization by means of Hubbard–Stratonovich transformations. To this end, we

introduce the auxiliary meson fields $\sigma$, $\vec{\pi}$ and $\omega_\mu$ in the scalar, pseudoscalar and vector channel, respectively, as well as the complex auxiliary scalar diquark fields $\Delta_A$ and their complex conjugate fields $\Delta_A^*$. Then, after introducing Nambu–Gorkov bispinors

$$\Psi \equiv \frac{1}{\sqrt{2}}\begin{pmatrix} q \\ q^c \end{pmatrix} \qquad \bar{\Psi} \equiv \frac{1}{\sqrt{2}}\begin{pmatrix} \bar{q} & \bar{q}^c \end{pmatrix} \tag{9}$$

the grand partition function takes the form

$$\begin{aligned} \mathcal{Z} = & \int \mathscr{D}\sigma \mathscr{D}\vec{\pi} \mathscr{D}\omega_\mu \mathscr{D}\Delta_A \mathscr{D}\Delta_A^* \exp\left[\int \mathrm{d}^4 x_E \left(-\frac{\sigma^2+\vec{\pi}^2}{4G_S} - \frac{\Delta_A^*\Delta_A}{4G_D}\right)\right] \\ & \times \int \mathscr{D}\Psi \mathscr{D}\bar{\Psi} \exp\left[\int \mathrm{d}^4 \mathbf{x_E}\, \bar{\Psi}\, S^{-1} \Psi\right], \end{aligned} \tag{10}$$

with the inverse Nambu–Gorkov propagator defined as

$$S^{-1} \equiv \begin{pmatrix} \mathrm{i}\partial\!\!\!/ + \mu\gamma_0 + \gamma^\mu\omega_\mu - m_0 - \sigma - \mathrm{i}\gamma_5\vec{\tau}\cdot\vec{\pi} & \mathrm{i}\Delta_A\gamma_5\tau_2\lambda_A \\ \mathrm{i}\Delta_A^*\gamma_5\tau_2\lambda_A & \mathrm{i}\partial\!\!\!/ - \mu\gamma_0 - \gamma^\mu\omega_\mu - m_0 - \sigma - \mathrm{i}\gamma_5\vec{\tau}^T\cdot\vec{\pi} \end{pmatrix}. \tag{11}$$

Since the functional integral over the bispinor fields is of Gaussian type the quark degrees of freedom can be integrated out and we are able to express the partition function in terms of collective fields only, *viz.,*

$$\mathscr{Z} = \int \mathscr{D}\sigma\, \mathcal{D}\vec{\pi}\, \mathscr{D}\omega_\mu \mathscr{D}\Delta_A \mathcal{D}\Delta_A^*\, \mathrm{e}^{-\int \mathrm{d}^4 x_E \left\{ \frac{\sigma^2+\vec{\pi}^2}{4G_S} - \frac{\omega_\mu^2}{4G_V} + \frac{|\Delta_A|^2}{4G_D} \right\} + \frac{1}{2}\ln\det(\beta S^{-1})}. \tag{12}$$

The determinant is to be taken over Dirac, flavor, color and Nambu–Gorkov indices as well as over Euclidean 4-volume. The latter is accomplished after Fourier transforming the inverse quark propagator to the momentum space and Matsubara representation given by

$$S^{-1} = \begin{pmatrix} (\mathrm{i}z_n + \mu^*)\gamma_0 - \boldsymbol{\gamma}\cdot(\mathbf{p}+\boldsymbol{\omega}) - m - \mathrm{i}\gamma_5\vec{\tau}\cdot\vec{\pi} & \Delta_A \mathrm{i}\gamma_5\tau_2\lambda_A \\ \Delta_A^* \mathrm{i}\gamma_5\tau_2\lambda_A & (\mathrm{i}z_n - \mu^*)\gamma_0 - \boldsymbol{\gamma}\cdot(\mathbf{p}-\boldsymbol{\omega}) - m - \mathrm{i}\gamma_5\vec{\tau}^{\,T}\cdot\vec{\pi} \end{pmatrix} \tag{13}$$

with $z_n = (2n+1)\pi T$ being fermionic Matsubara frequencies. Bold-face symbols denote space-like components of four-vectors and gamma matrices, and the transposed isospin matrices are given by $\vec{\tau}^{\,T} = (\tau_1, -\tau_2, \tau_3)$. Finally, we have introduced the combinations

$$m = m_0 + \sigma, \qquad \mu^* = \mu + \omega_0, \tag{14}$$

which can be interpreted as an effective (constituent) quark mass and an effective chemical potential.

### 2.1. Mean-field approximation

To proceed further, we employ the homogeneous mean-field approximation, *i.e.,* we replace all occurring fields by homogeneous and isotropic mean fields. Then the functional integration in Eq. (12) becomes trivial, and the partition function essentially factorizes into a Gaussian part and a contribution from the inverse quark propagator. Accordingly, the thermodynamic potential per volume, can be separated into a condensate part and a contribution from the quarks,

$$\Omega_{\mathrm{MF}} = \Omega_{\mathrm{cond}} + \Omega_{\mathrm{Q}}, \tag{15}$$

with

$$\Omega_{\mathrm{cond}} = \frac{\sigma_{\mathrm{MF}}^2}{4G_S} + \frac{|\Delta_{\mathrm{MF}}|^2}{4G_D} - \frac{\omega_{\mathrm{MF}}^2}{4G_V} \tag{16}$$

and

$$\Omega_{\mathrm{Q}} = -\frac{1}{2}\frac{T}{V}\mathrm{Tr}\ln\left(\beta S_{\mathrm{MF}}^{-1}\right). \tag{17}$$

Here the functional trace symbol Tr stands for summation over Matsubara frequencies and three-momenta as well as for the trace over internal degrees of freedom, *i.e.,* color, flavor, Dirac and Nambu–Gorkov space. The extra factor of $\frac{1}{2}$ arises from the artificial doubling of the degrees of freedom in Nambu–Gorkov formalism.

The isotropy implies $\boldsymbol{\omega}_{\rm MF} = 0$, hence $\omega_{\rm MF}$ denotes the 0-th component only. Also, anticipating that pseudoscalar mean fields are disfavored at nonzero bare quark masses and vanishing isospin chemical potential, $\vec{\pi}_{\rm MF}$ vanishes as well, and therefore was dropped in Eq. (16). Moreover, we have taken the freedom to perform a global color rotation, so that in the diquark sector the only non-vanishing mean fields correspond to the $A = 2$ direction, meaning that only the first two quark colors (red and green) participate in the condensate, while the third color (blue) remains unpaired.

The inverse quark propagator then takes the form

$$S_{\rm MF}^{-1} = \begin{pmatrix} (\mathrm{i}z_n + \mu^*)\gamma_0 - \boldsymbol{\gamma}\cdot\mathbf{p} - m & \Delta_{\rm MF}\mathrm{i}\gamma_5\tau_2\lambda_2 \\ \Delta_{\rm MF}^*\mathrm{i}\gamma_5\tau_2\lambda_2 & (\mathrm{i}z_n - \mu^*)\gamma_0 - \boldsymbol{\gamma}\cdot\mathbf{p} - m \end{pmatrix}. \tag{18}$$

The inverse propagator can be inverted to obtain the propagator

$$S_{\rm MF} \equiv \begin{pmatrix} \mathbf{G}^+ & \mathbf{F}^- \\ \mathbf{F}^+ & \mathbf{G}^- \end{pmatrix}. \tag{19}$$

The resulting normal and anomalous Nambu–Gorkov components are

$$\mathbf{G}_{\mathbf{p}}^{\pm} = \sum_{s_p}\left(\sum_{t_p}\frac{t_p}{2E_{\mathbf{p}}^{\pm s_p}}\frac{t_pE_{\mathbf{p}}^{\pm s_p} - s_p\xi_{\mathbf{p}}^{\pm s_p}}{\mathrm{i}z_n - t_pE_{\mathbf{p}}^{\pm s_p}}\mathcal{P}_{rg} + \frac{1}{\mathrm{i}z_n + s_p\xi_{\mathbf{p}}^{\pm s_p}}\mathcal{P}_b\right)\Lambda_{\mathbf{p}}^{-s_p}\gamma_0, \tag{20}$$

$$\mathbf{F}_{\mathbf{p}}^{\pm} = \mathrm{i}\sum_{s_p,t_p}\frac{t_p}{2E_{\mathbf{p}}^{\pm s_p}}\frac{\Delta_{\rm MF}^{\pm}}{\mathrm{i}z_n - t_pE_{\mathbf{p}}^{\pm s_p}}\tau_2\lambda_2\Lambda_{\mathbf{p}}^{s_p}\gamma_5, \tag{21}$$

where $s_p$, $t_p = \pm 1$ and $(\Delta_{\rm MF}^+, \Delta_{\rm MF}^-) \equiv (\Delta_{\rm MF}^*, \Delta_{\rm MF})$. $\mathcal{P}_{rg} = \mathrm{diag}_c(1, 1, 0)$, and $\mathcal{P}_b = \mathrm{diag}_c(0, 0, 1)$ are color projection operators, and $\Lambda_{\mathbf{p}}^{\pm} = [1 \pm \gamma_0(\boldsymbol{\gamma}\cdot\mathbf{p} + m)/E_{\mathbf{p}}]/2$ are projectors on positive and negative energy states, respectively. The corresponding quasi-particle dispersion relations are

$$\xi_{\mathbf{p}}^{\pm} = E_{\mathbf{p}} \pm \mu^* \tag{22}$$

for the blue quarks and

$$E_{\mathbf{p}}^{\pm} = \sqrt{(\xi_{\mathbf{p}}^{\pm})^2 + |\Delta_{\rm MF}|^2} \tag{23}$$

for the red and green quarks, where $E_{\mathbf{p}} = \sqrt{|\mathbf{p}|^2 + m^2}$.

The mean-field values are obtained as stationary points of the thermodynamic potential, *i.e.,*

$$0 = \frac{\partial\Omega_{\rm MF}}{\partial\sigma_{\rm MF}} = \frac{\sigma_{\rm MF}}{2G_{\rm S}} - \frac{1}{2}\frac{T}{V}\mathrm{Tr}\left(S_{\rm MF}\frac{\partial S_{\rm MF}^{-1}}{\partial\sigma_{\rm MF}}\right), \tag{24}$$

$$0 = \frac{\partial\Omega_{\rm MF}}{\partial\omega_{\rm MF}} = -\frac{\omega_{\rm MF}}{2G_{\rm V}} - \frac{1}{2}\frac{T}{V}\mathrm{Tr}\left(S_{\rm MF}\frac{\partial S_{\rm MF}^{-1}}{\partial\omega_{\rm MF}}\right), \tag{25}$$

$$0 = \frac{\partial\Omega_{\rm MF}}{\partial\Delta_{\rm MF}^*} = \frac{\Delta_{\rm MF}}{4G_{\rm D}} - \frac{1}{2}\frac{T}{V}\mathrm{Tr}\left(S_{\rm MF}\frac{\partial S_{\rm MF}^{-1}}{\partial\Delta_{\rm MF}^*}\right), \tag{26}$$

$$0 = \frac{\partial\Omega_{\rm MF}}{\partial\Delta_{\rm MF}} = \frac{\Delta_{\rm MF}^*}{4G_{\rm D}} - \frac{1}{2}\frac{T}{V}\mathrm{Tr}\left(S_{\rm MF}\frac{\partial S_{\rm MF}^{-1}}{\partial\Delta_{\rm MF}}\right). \tag{27}$$

The derivatives of the inverse propagator basically reduce to the vertex functions,

$$\frac{\partial S_{\rm MF}^{-1}}{\partial \sigma_{\rm MF}} = -\begin{pmatrix} 1 & 0 \\ 0 & 1 \end{pmatrix}, \qquad \frac{\partial S_{\rm MF}^{-1}}{\partial \omega_{\rm MF}} = \begin{pmatrix} \gamma^0 & 0 \\ 0 & -\gamma^0 \end{pmatrix}, \tag{28}$$

$$\frac{\partial S_{\rm MF}^{-1}}{\partial \Delta_{\rm MF}^*} = \begin{pmatrix} 0 & 0 \\ {\rm i}\gamma_5\lambda_2\tau_2 & 0 \end{pmatrix}, \qquad \frac{\partial S_{\rm MF}^{-1}}{\partial \Delta_{\rm MF}} = \begin{pmatrix} 0 & {\rm i}\gamma_5\lambda_2\tau_2 \\ 0 & 0 \end{pmatrix}, \tag{29}$$

and after performing the trace in Nambu–Gorkov space the gap equations become

$$\sigma_{\rm MF} = -G_{\rm S}\frac{T}{V}{\rm tr}\left(G_{\mathbf{p}}^+ + G_{\mathbf{p}}^-\right), \tag{30}$$

$$\omega_{\rm MF} = -G_{\rm V}\frac{T}{V}{\rm tr}\left[\left(G_{\mathbf{p}}^+ - G_{\mathbf{p}}^-\right)\gamma_0\right], \tag{31}$$

$$\Delta_{\rm MF} = 2G_{\rm D}\frac{T}{V}{\rm tr}\left[F_{\mathbf{p}}^-{\rm i}\gamma_5\tau_2\lambda_2\right], \tag{32}$$

$$\Delta_{\rm MF}^* = 2G_{\rm D}\frac{T}{V}{\rm tr}\left[F_{\mathbf{p}}^+{\rm i}\gamma_5\tau_2\lambda_2\right], \tag{33}$$

where tr denotes the remaining functional trace. Carrying out the trace in color, flavor and Dirac space and performing the sum over Matsubara frequencies using

$$T\sum_n \frac{1}{{\rm i}z_n - x} = n(x), \tag{34}$$

with $n(x) = [\exp(x/T)+1]^{-1}$ being the Fermi distribution function, we finally obtain

$$\begin{aligned} m - m_0 \;=\; & 4N_f G_{\rm S} m \int \frac{{\rm d}^3p}{(2\pi)^3}\frac{1}{E_{\mathbf{p}}}\left\{\left[1-2n(E_{\mathbf{p}}^-)\right]\frac{\xi_{\mathbf{p}}^-}{E_{\mathbf{p}}^-}\right. \\ & \left. + \left[1-2n(E_{\mathbf{p}}^+)\right]\frac{\xi_{\mathbf{p}}^+}{E_{\mathbf{p}}^+} + n(-\xi_{\mathbf{p}}^+) - n(\xi_{\mathbf{p}}^-)\right\}, \end{aligned} \tag{35}$$

$$\mu - \mu^* = 4N_f G_{\rm V}\int \frac{{\rm d}^3p}{(2\pi)^3}\left[[1-2n(E_{\mathbf{p}}^+)]\frac{\xi_{\mathbf{p}}^+}{E_{\mathbf{p}}^+} - [1-2n(E_{\mathbf{p}}^-)]\frac{\xi_{\mathbf{p}}^-}{E_{\mathbf{p}}^-} + n(\xi_{\mathbf{p}}^-) - n(\xi_{\mathbf{p}}^+)\right], \tag{36}$$

$$\Delta_{\rm MF} = 4N_f G_{\rm D}\Delta_{\rm MF}\int \frac{{\rm d}^3p}{(2\pi)^3}\left[\frac{1-2n(E_{\mathbf{p}}^-)}{E_{\mathbf{p}}^-} + \frac{1-2n(E_{\mathbf{p}}^+)}{E_{\mathbf{p}}^+}\right]. \tag{37}$$

For $\Delta_{\rm MF}^*$ one gets just the complex conjugate of Eq. (37). Moreover, only the modulus of $\Delta_{\rm MF}$ is fixed by the gap equations, while the choice of the phase is arbitrary. In practice, $\Delta_{\rm MF}$ is therefore usually chosen to be real. However, the complex nature of the diquark field must be kept in mind when fluctuations are taken into account.

The corresponding thermodynamic potential is then readily evaluated to

$$\begin{aligned} \Omega_{\rm MF} = \; & \frac{\sigma_{\rm MF}^2}{4G_{\rm S}} - \frac{\omega_{\rm MF}^2}{4G_{\rm V}} + \frac{|\Delta_{\rm MF}|^2}{4G_{\rm D}} - 2N_f\int\frac{{\rm d}^3p}{(2\pi)^3}[E_{\mathbf{p}}^+ + 2T\ln(1+{\rm e}^{-E_{\mathbf{p}}^+/T}) \\ & + E_{\mathbf{p}}^- + 2T\ln(1+{\rm e}^{-E_{\mathbf{p}}^-/T}) + E_{\mathbf{p}} + T\ln(1+{\rm e}^{-\xi_{\mathbf{p}}^+/T}) + T\ln(1+{\rm e}^{-\xi_{\mathbf{p}}^-/T})]. \end{aligned} \tag{38}$$

In general the gap equations have more than one solution. The stable solution is then the set of self-consistent mean fields which minimizes the thermodynamic potential. For the standard choice of attractive scalar quark–antiquark and quark–quark interactions and repulsive vector interactions, this solution corresponds to a minimum w.r.t. $\sigma_{\rm MF}$ and $\Delta_{\rm MF}$, but to a maximum w.r.t. $\omega_{\rm MF}$. The latter is just a constraint for thermodynamic consistency.

The above expressions get strongly simplified in the non-superconducting ("normal") phase, where the diquark condensates vanish, $\Delta_{\rm MF} = 0$. In this case, the remaining gap equations reduce to

$$m - m_0 = 4N_f N_c G_S \int \frac{{\rm d}^3p}{(2\pi)^3} \frac{m}{E_{\mathbf{p}}} \left[1 - n(\xi_{\mathbf{p}}^+) - n(\xi_{\mathbf{p}}^-)\right], \tag{39}$$

$$\mu - \mu^* = 4N_f N_c G_V \int \frac{{\rm d}^3p}{(2\pi)^3} \left[n(\xi_{\mathbf{p}}^-) - n(\xi_{\mathbf{p}}^+)\right], \tag{40}$$

while the thermodynamic potential becomes

$$\Omega_{\rm MF} = \frac{\sigma_{\rm MF}^2}{4G_S} - \frac{\omega_{\rm MF}^2}{4G_V} - 2N_f N_c \int \frac{{\rm d}^3p}{(2\pi)^3} \times \left[E_{\mathbf{p}} + T \ln\left(1 + {\rm e}^{-(E_{\mathbf{p}} - \mu^*)/T}\right) + T \ln\left(1 + {\rm e}^{-(E_{\mathbf{p}} + \mu^*)/T}\right)\right]. \tag{41}$$

The prefactors $N_f$, $N_c$ are obtained naturally from the color and flavor traces and are a consequence of persisting isospin and color symmetry.

### 2.2. Beyond mean field: Gaussian approximation

In mean-field approximation the thermodynamic potential corresponds to a Fermi gas of quasi-particles with dispersion relations which could be strongly modified compared to the non-interacting case by the various mean fields. On the other hand, the effects of low-lying bosonic excitations, in particular of the Goldstone bosons of the spontaneously broken symmetries, are completely missing. This could be a rather bad approximation at low temperatures, where the excitation of the fermionic quasi-particles is strongly suppressed by large constituent quark masses or pairing gaps, so that the Goldstone bosons are the dominant degrees of freedom.

In this section we therefore allow for fluctuations of the meson and diquark fields around their mean-field values and derive their contributions to the thermodynamic potential. In this article, we will fix the order parameters on the mean-field level only, *i.e.,* by the gap equations derived in the previous subsection. Eventually, one should derive the generalized gap equations, where the fluctuation corrections to the mean-field thermodynamic potential are taken into account in the minimization procedure.

We slightly change our notation in the $\sigma$ and $\omega_0$ channels and introduce shifted fields,

$$\sigma \to \sigma_{\rm MF} + \sigma, \tag{42}$$

$$\omega_0 \to \omega_{\rm MF} + \omega_0, \tag{43}$$

so that, from now on, $\sigma$ and $\omega_0$ denote only the fluctuating parts of the fields. Obviously, this is also true for the meson fields with vanishing mean fields, *i.e.,* pions and the space-like components of the $\omega$. For the diquarks we write

$$\Delta_2 = \Delta_{\rm MF} + \delta_2, \qquad \Delta_5 \equiv \delta_5, \qquad \Delta_7 \equiv \delta_7, \tag{44}$$

and analogously for the complex conjugate fields.

The Gaussian terms in the partition function, Eq. (12), are then to be replaced by

$$\sigma^2 + \vec{\pi}^{\,2} \to \sigma_{\rm MF}^2 + 2\sigma_{\rm MF}\sigma + \sigma^2 + \vec{\pi}^{\,2}, \tag{45}$$

$$\omega_\mu^2 \to \omega_{\rm MF}^2 + 2\omega_{\rm MF}\omega_0 + \omega_\mu^2, \tag{46}$$

$$|\Delta_A|^2 = |\Delta_{\rm MF}|^2 + \Delta_{\rm MF}\delta_2^* + \Delta_{\rm MF}^*\delta_2 + |\delta_A|^2, \tag{47}$$

where a sum over the indices $\mu$ and $A$ was implied, as before.

In addition, the fluctuations contribute to the partition function via the inverse propagator, which can be written as

$$S^{-1} = S_{\rm MF}^{-1} + \Sigma, \tag{48}$$

with

$$\Sigma = \begin{pmatrix} \gamma^\mu\omega_\mu - \sigma - \mathrm{i}\gamma_5\vec{\tau}\cdot\vec{\pi} & \delta_A \mathrm{i}\gamma_5\tau_2\lambda_A \\ \delta_A^*\mathrm{i}\gamma_5\tau_2\lambda_A & -\gamma^\mu\omega_\mu - \sigma - \mathrm{i}\gamma_5\vec{\tau}^{\,T}\cdot\vec{\pi} \end{pmatrix}. \tag{49}$$

The logarithmic term in Eq. (12) then takes the form

$$\ln\det\left(\beta S^{-1}\right) = \mathrm{Tr}\ln\left(\beta S_{\mathrm{MF}}^{-1} + \beta\Sigma\right) = \mathrm{Tr}\ln\left(\beta S_{\mathrm{MF}}^{-1}\right) + \mathrm{Tr}\ln(1 + S_{\mathrm{MF}}\Sigma) \tag{50}$$

and can be Taylor-expanded in the fluctuating fields. Here we expand it up to quadratic (Gaussian) order as to account for two-particle correlations. Higher-order correlations will be ignored and are left to a later investigation. Those correlations would include baryons. We obtain

$$\ln\det\left(\beta S^{-1}\right) = \mathrm{Tr}\ln\left(\beta S_{\mathrm{MF}}^{-1}\right) + \mathrm{Tr}\left(S_{\mathrm{MF}}\Sigma - \frac{1}{2}S_{\mathrm{MF}}\Sigma S_{\mathrm{MF}}\Sigma\right) + \mathscr{O}\left(\Sigma^3\right), \tag{51}$$

and the partition function in Gaussian approximation neglecting contributions $\mathscr{O}\left(\Sigma^3\right)$ can be written as

$$\mathscr{Z}_{\mathrm{Gauß}} = \mathscr{Z}_{\mathrm{MF}} \int \mathscr{D}\sigma\,\mathscr{D}\vec{\pi}\,\mathscr{D}\omega_\mu\,\mathscr{D}\delta_A\mathscr{D}\delta_A^*\,\mathrm{e}^{\mathscr{A}^{(1)}+\mathscr{A}^{(2)}} \tag{52}$$

with the mean-field partition function $\mathscr{Z}_{\mathrm{MF}} = \exp\left(-\beta V\Omega_{\mathrm{MF}}\right)$, and two correction terms to the Euclidean action which are linear and quadratic in the fluctuations, *viz.*,

$$\mathscr{A}^{(1)} = -\beta V\left(\frac{\sigma_{\mathrm{MF}}\sigma}{2G_{\mathrm{S}}} + \frac{\Delta_{\mathrm{MF}}\delta_2^* + \Delta_{\mathrm{MF}}^*\delta_2}{4G_{\mathrm{D}}} - \frac{\omega_{\mathrm{MF}}\omega_0}{2G_{\mathrm{V}}}\right) + \frac{1}{2}\mathrm{Tr}\left[S_{\mathrm{MF}}\Sigma\right], \tag{53}$$

and

$$\mathscr{A}^{(2)} = -\beta V\left(\frac{\sigma^2+\vec{\pi}^2}{4G_{\mathrm{S}}} + \frac{|\delta_A|^2}{4G_{\mathrm{D}}} - \frac{\omega_\mu^2}{4G_{\mathrm{V}}}\right) - \frac{1}{4}\mathrm{Tr}\left[S_{\mathrm{MF}}\Sigma S_{\mathrm{MF}}\Sigma\right]. \tag{54}$$

The linear correction term vanishes as a result of the mean-field gap equations. To show this, we evaluate the Nambu–Gorkov trace of the last term in Eq. (53),

$$\begin{aligned} -\mathrm{Tr}\left[S_{\mathrm{MF}}\Sigma\right] = \frac{1}{2}\mathrm{tr}[&G_{\mathbf{p}}^+(\sigma + \mathrm{i}\gamma_5\vec{\tau}\cdot\vec{\pi} - \gamma^\mu\omega_\mu) + G_{\mathbf{p}}^-(\sigma + \mathrm{i}\gamma_5\vec{\tau}^{\,T}\cdot\vec{\pi} + \gamma^\mu\omega_\mu) \\ &- F_{\mathbf{p}}^+\delta_A\mathrm{i}\gamma_5\tau_2\lambda_A - F_{\mathbf{p}}^-\delta_A^*\mathrm{i}\gamma_5\tau_2\lambda_A]. \end{aligned} \tag{55}$$

The pion fields and the space-like $\omega$-components drop out in the subsequent flavor trace and momentum integral, respectively, as the normal propagator components, given in Eq. (20), respect the isospin symmetry and the isotropy of the medium. Similarly, the $A = 5, 7$ diquark fields drop out in the color trace. The remaining terms are canceled by the other terms in Eq. (53), which can be seen easily when we group them together field-wise and use the gap equations (30)–(33) to obtain

$$\frac{1}{2}\left(\frac{\sigma_{\mathrm{MF}}}{G_{\mathrm{S}}} + \frac{T}{V}\mathrm{tr}\left(G_{\mathbf{p}}^+ + G_{\mathbf{p}}^-\right)\right)\sigma = 0 \tag{56}$$

$$\frac{1}{2}\left(-\frac{\omega_{\mathrm{MF}}}{G_{\mathrm{V}}} - \frac{T}{V}\mathrm{tr}\left[\left(G_{\mathbf{p}}^+ - G_{\mathbf{p}}^-\right)\gamma_0\right]\right)\omega_0 = 0 \tag{57}$$

$$\frac{1}{2}\left(\frac{\Delta_{\mathrm{MF}}}{2G_{\mathrm{D}}} - \frac{T}{V}\mathrm{tr}\left[F_{\mathbf{p}}^-\mathrm{i}\gamma_5\tau_2\lambda_2\right]\right)\delta_2^* = 0 \tag{58}$$

$$\frac{1}{2}\left(\frac{\Delta_{\mathrm{MF}}^*}{2G_{\mathrm{D}}} - \frac{T}{V}\mathrm{tr}\left[F_{\mathbf{p}}^+\mathrm{i}\gamma_5\tau_2\lambda_2\right]\right)\delta_2 = 0. \tag{59}$$

Hence, the partition function reads

$$\mathscr{Z}_{\mathrm{Gauß}} = \mathscr{Z}_{\mathrm{MF}} \int \mathcal{D}\sigma\,\mathcal{D}\vec{\pi}\,\mathcal{D}\omega_\mu\,\mathcal{D}\delta_A\mathcal{D}\delta_A^*\,\mathrm{e}^{\mathscr{A}^{(2)}}. \tag{60}$$

By construction, the exponent is bilinear in the fields, so that the path integrals can be carried out. To that end, we combine all fields in a vector

$$X = \begin{pmatrix} \vec{\pi} \\ \omega_\mu \\ \sigma \\ \delta_A \\ \delta_A^* \end{pmatrix}, \qquad X^\dagger = (\vec{\pi}^{\,T}, \omega_\mu, \sigma, \delta_A^*, \delta_A), \tag{61}$$

where all vector-meson components $\mu$ and all diquark fields, $A = 2, 5, 7$, are implied, as it was in the partition function. The trace in the exponent can then be written as

$$\frac{1}{2}\mathrm{Tr}[S_{\rm MF}\Sigma S_{\rm MF}\Sigma] = -X^\dagger \Pi X, \tag{62}$$

with the polarization matrix $\Pi$. In addition, we have the Gaussian terms in front of the trace, which are diagonal in this basis. Combining both parts, we write

$$\frac{\sigma^2 + \vec{\pi}^2}{2G_{\rm S}} + \frac{|\delta_A|^2}{2G_{\rm D}} - \frac{\omega_\mu^2}{2G_{\rm V}} + \frac{1}{2}\frac{T}{V}\mathrm{Tr}[S_{\rm MF}\Sigma S_{\rm MF}\Sigma] = X^\dagger \tilde{S}^{-1} X, \tag{63}$$

with a, in general non-diagonal, propagator matrix $\tilde{S}$. The partition function is then readily evaluated as

$$\mathscr{Z}_{\rm Gauß} = \mathscr{Z}_{\rm MF} \int \mathscr{D}X\, \mathrm{e}^{-\frac{1}{2}\int \mathrm{d}^4x_E \left\{X^\dagger \tilde{S}^{-1} X\right\}} = \mathscr{Z}_{\rm MF} \left[\det\left(\beta^2 \tilde{S}^{-1}\right)\right]^{-1/2}. \tag{64}$$

Note that for evaluating the Gaussian functional integrals over the set of bosonic fields forming the components of the vector $X$ we performed a Fourier transformation of these fields to their representation in the space of three-momenta and Matsubara frequencies where they are normalized to be dimensionless, see Chapter 2.3 of [41]. After diagonalizing $\tilde{S}^{-1}$, the partition function factorizes,

$$\mathscr{Z}_{\rm Gauß} = \mathscr{Z}_{\rm MF} \prod_X \mathscr{Z}_X, \tag{65}$$

with $\mathscr{Z}_X = \left[\det\left(\beta^2 S_X^{-1}\right)\right]^{-d_X/2}$ being the partition function related to the propagator $S_X$ of the $d_X$-fold degenerate eigenmode $X$ operating in the $d_X$-dimensional subspace of the general propagator $\tilde{S}$ of two-quark correlations. Accordingly, the thermodynamic potential becomes a sum of the mean-field part and the fluctuation parts related to these modes,

$$\Omega_{\rm Gauß} = -\frac{T}{V}\ln \mathscr{Z}_{\rm Gauß} = \Omega_{\rm MF} + \Omega^{(2)} = \Omega_{\rm cond} + \Omega_{\rm Q} + \sum_X \Omega_X, \tag{66}$$

with

$$\Omega_X(T,\mu) = \frac{d_X}{2}\frac{T}{V}\mathrm{Tr}\ln\left[\beta^2 S_X^{-1}(\mathrm{i}z_n, \mathbf{q})\right], \tag{67}$$

where Tr stands for summation over 3-momenta and Matsubara frequencies of the bosonic two-particle correlation in the channel $X$.

The elements of the polarization matrix $\Pi$ are explicitly listed in Appendix for the simplified case where the vector fields $\omega_\mu$ have been neglected. In the 2SC phase, *i.e.,* for $\Delta_{\rm MF} \neq 0$, the $\sigma$-meson mode mixes with the diquark modes $\delta_2$ and $\delta_2^*$, formally evident from the occurrence of non-diagonal elements in the polarization matrix. Physically, this reflects the non-conservation of baryon number in the superfluid medium.

In the non-superconducting phase where $\Delta_{\rm MF} = 0$, on the other hand, baryon number is conserved and meson, diquark and anti-diquark modes decouple,

$$\Omega_{\rm Gauß} = \Omega_{\rm cond} + \Omega_{\rm Q} + \Omega_{\rm M} + \Omega_{\rm D} + \Omega_{\bar{\rm D}}. \tag{68}$$

The three diquark modes $D = \delta_A$, related to $A = 2, 5, 7$, are degenerate because of the persisting color symmetry, whereas the chemical potential causes a splitting between diquarks and anti-diquarks, $\Omega_{\bar{\rm D}}(T,\mu) = \Omega_{\rm D}(T,-\mu)$. In the meson sector, the pions always decouple from the scalar and vector modes because of parity and angular momentum conservation. On the other hand, the $\omega_0$-mode can mix with the $\sigma$ at nonzero $\mu$.

Neglecting again the vector fields, all elementary meson and diquark modes of the original Lagrangian decouple in the normal phase,

$$\Omega_{\rm Gauß} = \Omega_{\rm cond} + \Omega_{\rm Q} + \Omega_\sigma + \Omega_\pi + \Omega_{\rm D} + \Omega_{\bar{\rm D}}, \tag{69}$$

and the correlation contributions from the composite fields are determined by

$$\Omega_X(T,\mu) = \frac{d_X}{2} T \sum_n \int \frac{{\rm d}^3 q}{(2\pi)^3} \ln\left[\beta^2 S_X^{-1}({\rm i}z_n, \mathbf{q})\right]$$

$$S_X^{-1}({\rm i}z_n, \mathbf{q}) = \frac{1}{G_X} - \Pi_X({\rm i}z_n, \mathbf{q}). \tag{70}$$

Here $G_X$ is the coupling, related to the channel $X$, *i.e.*, $G_X = 2G_{\rm S}$ for $X = \sigma, \pi$ and $G_X = 2G_D$ for $X = \delta_A, \delta_A^*$, and $\Pi_X$ denotes the diagonal element of the polarization matrix in this channel. The corresponding degeneracy factors $d_X$ are $d_\sigma = 1$ for the sigma meson and $d_\pi = d_D = d_{\bar{D}} = 3$ for pions, diquarks and anti-diquarks, respectively.

## 3. Meson and diquark spectra and their mixing in the 2SC phase

In this section, we want to discuss the meson and diquark spectra, which are given by the poles of the propagator matrix, *i.e.*, by the zeros of $\det \tilde{S}^{-1}$. In the normal phase, this is simplified by the fact that the various meson and diquark modes separate, as mentioned above. In the 2SC phase, on the other hand, the polarization matrix has non-diagonal elements which cause a mixing of the $\sigma$ mode with the $A = 2$ diquarks and anti-diquarks. Therefore, we will mainly concentrate on this mixing.

The relevant piece of the inverse propagator matrix has the form

$$\tilde{S}^{-1}_{\rm mix} \equiv \begin{pmatrix} S^{-1}_{\sigma\sigma} & S^{-1}_{\sigma\delta_2} & S^{-1}_{\sigma\delta_2^*} \\ S^{-1}_{\delta_2^*\sigma} & S^{-1}_{\delta_2^*\delta_2} & S^{-1}_{\delta_2^*\delta_2^*} \\ S^{-1}_{\delta_2\sigma} & S^{-1}_{\delta_2\delta_2} & S^{-1}_{\delta_2\delta_2^*} \end{pmatrix} = \begin{pmatrix} \frac{1}{2G_{\rm S}} - \Pi_{\sigma\sigma} & -\Pi_{\sigma\delta_2} & -\Pi_{\sigma\delta_2^*} \\ -\Pi_{\delta_2^*\sigma} & \frac{1}{4G_{\rm D}} - \Pi_{\delta_2^*\delta_2} & -\Pi_{\delta_2^*\delta_2^*} \\ -\Pi_{\delta_2\sigma} & -\Pi_{\delta_2\delta_2} & \frac{1}{4G_{\rm D}} - \Pi_{\delta_2\delta_2^*} \end{pmatrix}, \tag{71}$$

with the polarization-matrix elements given in Appendix. These matrix elements and therefore also the elements of the inverse propagator matrix depend on an external three-momentum $\mathbf{q}$ and an external bosonic Matsubara frequency $z_n$. In the following both functions will be analytically continued to the complex plane, replacing ${\rm i}z_n$ by the complex variable $z$.

In order to determine the eigenmodes, $\tilde{S}^{-1}_{\rm mix}$ needs to be diagonalized. Thereby we will restrict ourselves to mesons and diquarks which are at rest in the medium, $\mathbf{q} = 0$. Then, as shown in Appendix A.2, the polarization matrix elements simplify dramatically. Combining them with the diagonal coupling terms, we have

$$S^{-1}_{\sigma\sigma}(z) = \frac{1}{2G_{\rm S}} + 8I_\sigma(z) + 16m^2|\Delta_{\rm MF}|^2 I_4(z) \tag{72}$$

$$S^{-1}_{\delta_2\delta_2}(z) = -4\Delta^2_{\rm MF} I_0(z) \tag{73}$$

$$S^{-1}_{\delta_2^*\delta_2}(z) = \frac{1}{4G_{\rm D}} - 2I_\Delta - 4zI_1(z) - \left(4|\Delta_{\rm MF}|^2 - 2z^2\right) I_0(z) \tag{74}$$

$$S^{-1}_{\sigma\delta_2}(z) = 4m\Delta_{\rm MF}\left(zI_2(z) + 2I_3(z)\right), \tag{75}$$

while the remaining elements of $\tilde{S}^{-1}_{\rm mix}$ follow from the symmetry relations Eqs. (A.9)–(A.13). Here we have dropped the three-momentum argument, $\mathbf{q} = 0$, for brevity. The constant $I_\Delta$ and the functions $I_i(z)$ are the finite-temperature extensions of the integrals introduced in Ref. [42] and are explicitly given in Appendix A.2.

The above expressions are general and valid in all phases. In particular, we see that the mixing terms vanish in the normal phase, where $\Delta_{\rm MF} = 0$. In the 2SC phase, where the mixing persists, it is more tedious, but straightforward to calculate the determinant of $\tilde{S}^{-1}_{\rm mix}$. The corresponding eigenmodes, *i.e.,* the zeros of the determinant must in general be determined numerically.

An exception is the Goldstone modes in the 2SC phase, which can be found analytically. These modes are related to the spontaneous breaking of the color SU(3) symmetry down to SU(2). In this context we remind that the color symmetry is a global symmetry in the present model. In QCD, where it is a local gauge symmetry, the would-be Goldstone modes, which are related to the five generators of the broken symmetry are "eaten" by five gluons, giving them a non-zero Meissner mass. Hence, naively, one would expect that in the present model there are five Goldstone bosons in the 2SC phase. However, as shown in Ref. [43] there are in fact only three Goldstone bosons, with two of them having a quadratic dispersion relation, in agreement with the Nielsen–Chadha theorem [44]. This abnormal number of Goldstone bosons can be related to the nonzero color charge [43,45,46], which arises in the 2SC phase as a consequence of the fact that only red and green quarks are paired. (In QCD, the 2SC phase is always color neutralized by the background gluon field [47].)

In order to identify the Goldstone modes, we evaluate the matrix elements at $z = 0$. In this limit (and additionally choosing $\Delta_{\rm MF}$ to be a real quantity) we can make extensive use of the symmetry relations quoted in Eqs. (A.9)–(A.13), to show that the determinant can be written as

$$\det \tilde{S}^{-1}_{\rm mix} = \left(S^{-1}_{\delta_2\delta_2^*} - S^{-1}_{\delta_2\delta_2}\right)\left[S^{-1}_{\sigma\sigma}\left(S^{-1}_{\delta_2\delta_2^*} + S^{-1}_{\delta_2\delta_2}\right) - 2S^{-2}_{\sigma\delta_2}\right]. \tag{76}$$

Evaluating Eqs. (73) and (74) at $z = 0$ and using the 2SC gap equation,

$$1 = 8G_{\rm D}I_\Delta, \tag{77}$$

one then finds that the first term, $S^{-1}_{\delta_2\delta_2^*} - S^{-1}_{\delta_2\delta_2}$ vanishes, thus proving the existence of a Goldstone mode.

The mixing-problem gets strongly simplified if the quarks in the 2SC phase are strictly massless, which is the case in the chiral limit for a sufficiently weak diquark coupling $G_{\rm D}$. In this case the mixing between the $\sigma$ and the diquark and anti-diquark vanishes, see Eq. (75), *i.e.,* the mixing is restricted to the $A = 2$ diquark and anti-diquark sector. The determinant of the corresponding mixing matrix is then given by

$$\det \tilde{S}^{-1}_{{\rm mix},{\rm D}\bar{\rm D}}(z) = 4z^2[(z^2 - 4\Delta^2_{\rm MF})I_0(z)^2 - 4I_1(z)^2], \tag{78}$$

which makes the Goldstone mode at $z = 0$ explicit. In addition, it has a second root, which can be found by solving the self-consistent equation

$$z = 2\Delta_{\rm MF}\sqrt{1 + \left(\frac{I_1(z)}{\Delta_{\rm MF}I_0(z)}\right)^2}. \tag{79}$$

This solution is manifestly above the threshold for pair breaking $2\Delta_{\rm MF}$ and thus unstable.

The remaining Goldstone modes are found in the other color directions of the diquark sector, which do not mix. In these channels the inverse propagators read

$$S^{-1}_{\delta_5^*\delta_5}(z) = S^{-1}_{\delta_7^*\delta_7}(z) = \frac{1}{4G_{\rm D}} - I_\Delta - 2zI_7(z) + (|\Delta_{\rm MF}|^2 - z^2)I_5(z) \tag{80}$$

and $S^{-1}_{\delta_5\delta_5^*}(z) = S^{-1}_{\delta_7\delta_7^*}(z) = S^{-1}_{\delta_5^*\delta_5}(-z)$. Observing that $I_5(z = 0) = -I_\Delta/|\Delta_{\rm MF}|^2$ and using the gap equation again, one finds that these inverse propagators also vanish at $z = 0$.

A closer inspection shows that $\det \tilde{S}^{-1}_{\rm mix}$ yields a factor $z^2$ (as evident in the chiral limit from Eq. (78)), whereas $S^{-1}_{\delta_A\delta_A^*}(z)$ and $S^{-1}_{\delta_A^*\delta_A}$ in the $A = 5$ and 7 sectors only contribute a factor $z$ each, so that

diquarks and anti-diquarks must be combined to be counted as a full Goldstone mode. This leads to a total number of three Goldstone bosons, as already mentioned above.

For completeness, the pion propagator at rest is given by

$$S_{\pi\pi}^{-1}(z) = \frac{1}{2G_S} + 8I_\pi(z), \tag{81}$$

with the function $I_\pi(z)$ as defined in Eq. (A.33). As well known, in the chiral limit, the pions are the Goldstone bosons in the chirally broken normal phase ($m \neq 0$), while for $m = 0$, they become degenerate with the $\sigma$ meson.

Finally, we would like to point out that, in general, the pole energies of the eigenmodes at $\mathbf{q} = 0$ should not be called "masses", although this is quite common in the literature [48,49]. To see this, we recall that the propagator of a free boson with mass $m_X$ at boson-chemical potential $\mu_X$ has the form

$$S_X^{\rm free} = \frac{1}{(z+\mu_X)^2 - \mathbf{q}^2 - m_X^2}, \tag{82}$$

which, for $\mathbf{q} = 0$, has poles at $z = \pm m_X - \mu_X \equiv \omega_X^\pm$. Thus, we should identify the mass and the chemical potential of the bosonic mode $X$ from its pole energies as [50]

$$m_X = \frac{1}{2}(\omega_X^+ - \omega_X^-), \qquad \mu_X = -\frac{1}{2}(\omega_X^+ + \omega_X^-). \tag{83}$$

Of course, in the normal phase, the assignment of the chemical potentials corresponds to the net quark-number content of the boson, *i.e.*, $\mu_X = 0$ for the mesons, $\mu_X = 2\mu^*$ for the diquarks, and $\mu_X = -2\mu^*$ for the anti-diquarks. As a consequence, the poles of the diquark and anti-diquark propagators split, even at $T = 0$ and low chemical potentials (see, *e.g.*, Ref. [42]), while their true masses stay at their vacuum values until the lowest excitation threshold is reached or a phase transition takes place.

In the 2SC phase, on the other hand, where baryon number is not conserved and mixing takes place, the chemical potentials $\mu_X$ related to the various modes are less clear a priori and must be determined from Eq. (83).

## 4. Generalized Beth–Uhlenbeck equation of state

In the present section we will formulate the thermodynamics of two-particle correlations in a form which is known as the Beth–Uhlenbeck EoS [51,52]. The standard Beth–Uhlenbeck formula considers the second virial coefficient for the EoS that contains the contribution of bound states and scattering states in the low-density limit. In dense matter, the single-particle properties as well as the two-particle properties are modified. This is seen in the corresponding spectral functions where the $\delta$-like peaks describing the single-particle states and two-particle bound states (in the two-particle propagator) are shifted and broadened. The medium modifications of these quasiparticles are given in lowest approximation by the self-energy and (in the two-particle case) screening and Pauli-blocking contributions. When speaking of high densities we have in mind the occupation of phase space measured by scalar densities which can be large even at vanishing baryon density (zero chemical potential). We will generalize the standard Beth–Uhlenbeck approach to the situation in a hot and dense medium when the gap between the discrete spectrum of two-particle bound states and the scattering continuum (defining the binding energy) diminishes and finally vanishes so that the bound state merges the continuum. This generalized Beth–Uhlenbeck (GBU) EoS is applicable in a wide range of densities, improving the mean-field approach by including medium-modified two-particle correlations.

The dissolution of composite particles into their constituents because of the screening of interaction in a dense medium is known as the Mott effect in solid state physics and has also found numerous applications in semiconductor physics (transition from the exciton gas to the electron–hole liquid [53]), plasma physics (pressure ionization [54]) and nuclear physics (cluster dissociation due to Pauli blocking [55]). Here we want to apply the concept to particle physics and formulate the problem of hadron dissociation as a Mott effect. As it is known that this effect should not lead to discontinuities in the thermodynamic functions like the density, one has to take care of the normalization of the

spectral function of the two-particle correlations. Whenever a bound state gets dissociated, it should leave a trace in the behavior of the scattering phase shift at the threshold of the continuum. This constraint is known as Levinson's theorem II [56,57]. As we shall see, it can play an important role for the formulation of the thermodynamics of hadronic matter under extreme conditions where one of the key puzzles is the mechanism of hadron dissociation at the transition to the quark–gluon plasma (QGP) or, equivalently, the problem of hadronization of the QGP in the course of which correlations (pre-hadrons) form in the vicinity of the quark-to-hadron matter transition. Those correlations shall play a decisive role, *e.g.,* for understanding the chemical freeze-out. In the present section we will formulate the thermodynamics in the Beth–Uhlenbeck form [51,52] which allows the discussion of these issues in terms of two-particle correlations (2nd virial coefficient) as expressed by scattering phase shifts.

While in a low-density system, the phase shifts can be regarded as measurable quantities which then may be used to express deviations from an ideal gas behavior due to two-particle correlations in a dilute medium, the situation changes in a dense system. Under extreme conditions, in particular in the vicinity of the Mott transition, the modification of the two-particle system by the influence of the medium has to be taken into account. This has been done systematically within a thermodynamic Green function approach [58] but its extension for relativistic systems within a field theoretic formulation with contributions from anti-particles, relativistic kinematics and the role of the zero-point fluctuations has been missing. Previous work in this direction has been done by Hüfner et al. [21] and Abuki [59], who have chosen to introduce the scattering phase shifts as arguments of the Jost representation of the complex $\mathcal{S}$ matrix. Most recently, Wergieluk et al. [22], Yamazaki and Matsui [23], and Dubinin et al. [24] used a different approach where the phase shifts are encoding correlations of the relativistic two-particle propagators introduced above, which are the analogue of the $\mathcal{T}$ matrix of two-body scattering theory. Following this formalism, we thus develop here the field theoretic analogue of the approach by [53,58].

To be as transparent as possible in this basic and new contribution, we choose here to present derivations in the normal phase where $\Delta_{\rm MF} = 0$, neglecting the possibility of diquark condensation. The derivation of the more general case works in the same manner but involves the mathematical apparatus to deal with the mixing of correlation channels (see, e.g., [58]) which shall be given elsewhere. Note that the dissolution of composite particles into their constituents gives no discontinuities in the thermodynamic properties as long as homogeneous systems are considered. However, phase instabilities are provoked if the stability criteria according to the second law are violated due to the contribution of two-particle correlations to the EoS.

### 4.1. Bound states vs. continuum. Mott effect

Starting point for the derivation of the GBU EoS is the thermodynamic potential (69) which separates into the contributions from the eigenmodes of the two-particle propagation (70) as encoded in the two-particle propagators $S_X(\mathrm{i}z_n, \mathbf{q})$ with the inverse $S_X^{-1}(\mathrm{i}z_n, \mathbf{q}) = G_X^{-1} - \Pi_X(\mathrm{i}z_n, \mathbf{q})$ for a generic particle/correlation $X \in \{\mathrm{M}, \mathrm{D}\}$, defined at the Matsubara frequencies $\mathrm{i}z_n$. The complex function $S_X^{-1}(z, \mathbf{q})$ is its analytic continuation into the complex $z$-plane. $\Pi_X(\mathrm{i}z_n, \mathbf{q})$ is the polarization loop in the corresponding channel with an analytic continuation to the complex $z$-plane, analogous to that of the propagator. The complex propagator functions can be given the polar representation

$$S_X = |S_X|\, \mathrm{e}^{\mathrm{i}\delta_X} = S_R + \mathrm{i}S_I, \tag{84}$$

where the scattering phase shift $\delta_X$ has been introduced as

$$\delta_X(\omega, \mathbf{q}) = -\mathrm{Im}\ln\left[\beta^2 S_X^{-1}(\omega - \mu_X + \mathrm{i}\eta, \mathbf{q})\right]. \tag{85}$$

Note that in this definition we have shifted the energy argument in the inverse propagator by $-\mu_X$ in order to exploit the symmetry properties of the propagator, cf. Eq. (82). For the same reason, in the following discussion, the (inverse) propagator and the polarization function $\Pi_X$ should always be understood as to be evaluated at the shifted energy $z = \omega - \mu_X + \mathrm{i}\eta$, unless stated otherwise. Of course, this only concerns the diquarks and anti-diquarks, as for mesons we have $\mu_X = 0$ anyway.

The contribution of the mode $X$ to the thermodynamic potential as given in Eq. (67) can be transformed using the spectral representation of the function $\ln S_X^{-1}(\mathrm{i}z_n, \mathbf{q})$ and the definition of the phase shift (85) to obtain the form

$$\begin{aligned}\Omega_X(T,\mu) &= \frac{d_X}{2} T \sum_n \int \frac{\mathrm{d}^3 q}{(2\pi)^3} \ln\left[\beta^2 S_X^{-1}(\mathrm{i}z_n, \mathbf{q})\right], \\ &= -\frac{d_X}{2} T \sum_n \int \frac{\mathrm{d}^3 q}{(2\pi)^3} \int_{-\infty}^{\infty} \frac{\mathrm{d}\omega}{2\pi} \frac{2}{\mathrm{i}z_n - \omega} \mathrm{Im} \ln\left[\beta^2 S_X^{-1}(\omega + \mathrm{i}\eta, \mathbf{q})\right], \\ &= \frac{d_X}{2} T \sum_n \int \frac{\mathrm{d}^3 q}{(2\pi)^3} \int_{-\infty}^{\infty} \frac{\mathrm{d}\omega}{2\pi} \frac{2}{\mathrm{i}z_n - (\omega - \mu_X)} \delta_X(\omega, \mathbf{q}). \end{aligned} \tag{86}$$

Performing the bosonic Matsubara summation we arrive at

$$\Omega_X(T,\mu) = -d_X \int \frac{\mathrm{d}^3 q}{(2\pi)^3} \int_{-\infty}^{\infty} \frac{\mathrm{d}\omega}{2\pi} n_X^-(\omega) \delta_X(\omega, \mathbf{q}), \tag{87}$$

where we have employed the Bose function with chemical potential according to the notation $n_X^{\pm}(\omega) = 1/\{\exp[(\omega \pm \mu_X)/T] - 1\}$. After splitting the $\omega$-integration into negative and nonnegative domains and using the fact that for the Bose distribution function holds $n_X^-(-\omega) = -[1 + n_X^+(\omega)]$ while the phase shift (85) is an odd function under the reflection $\omega \to -\omega$ as a consequence of $J^{\pm}_{X,\mathrm{pair}}(-\omega) = -J^{\mp}_{X,\mathrm{pair}}(\omega)$ and $J^{\pm}_{X,\mathrm{Landau}}(-\omega) = -J^{\mp}_{X,\mathrm{Landau}}(\omega)$, see Appendices A.3 and A.4, we arrive at

$$\Omega_X(T,\mu) = -d_X \int \frac{\mathrm{d}^3 q}{(2\pi)^3} \int_0^{\infty} \frac{\mathrm{d}\omega}{2\pi} [1 + n_X^-(\omega) + n_X^+(\omega)] \delta_X(\omega, \mathbf{q}). \tag{88}$$

Here the shift in the definition of $\delta_X$, Eq. (85), was essential to have this symmetry property for diquarks and anti-diquarks as well. Performing a partial integration over the energy variable in (87) leads to

$$\begin{aligned}\Omega_X(T,\mu) = d_X \int \frac{\mathrm{d}^3 q}{(2\pi)^3} \int_0^{\infty} \frac{\mathrm{d}\omega}{2\pi} \left\{\omega + T \ln\left(1 - \mathrm{e}^{-(\omega-\mu_X)/T}\right) + T \ln\left(1 - \mathrm{e}^{-(\omega+\mu_X)/T}\right)\right\} \\ \times \frac{\mathrm{d}\delta_X(\omega, \mathbf{q})}{\mathrm{d}\omega}. \end{aligned} \tag{89}$$

This expression still contains the divergent vacuum energy contribution. We remove this term in analogy to the "no sea" approximation which is customary in relativistic mean field approaches to thermodynamics, like the Walecka model, and arrive at the Beth–Uhlenbeck formula for the pressure $p_X(T,\mu) = -\Omega_X(T,\mu)$,

$$\begin{aligned}p_X(T,\mu) = -d_X T \int \frac{\mathrm{d}^3 q}{(2\pi)^3} \int_0^{\infty} \frac{\mathrm{d}\omega}{2\pi} \left\{\ln\left(1 - \mathrm{e}^{-(\omega-\mu_X)/T}\right) + \ln\left(1 - \mathrm{e}^{-(\omega+\mu_X)/T}\right)\right\} \\ \times \frac{\mathrm{d}\delta_X(\omega, \mathbf{q})}{\mathrm{d}\omega}. \end{aligned} \tag{90}$$

With Eq. (90) the medium-dependent derivative of the phase shift $\delta_X'(\omega, \mathbf{q})$ has been introduced as a spectral weight factor for the contribution of a two-particle state $X$ with degeneracy factor $d_X$, depending on the three-momentum $\mathbf{q}$ and the two-particle energy $\omega$. Eq. (90) differs from the standard Beth–Uhlenbeck equation in nonrelativistic [52,51] or relativistic [57] systems by the fact that the two-particle propagator and therefore also the phase is obtained by taking into account in-medium effects as encoded in the solutions of the gap equations which define the quark quasiparticle (mean-field) propagators entering its definition.

Note that the phase angle used here should not be confused with an observable scattering phase shift which should be on the energy shell. Here the function $\delta_X(\omega, \mathbf{q})$ is merely a convenient parametrization of the spectral properties of the logarithm of the two-particle propagator $S_X(\omega - \mu_X +$

$\mathrm{i}\eta, \mathbf{q})$. The latter is defined by the polarization function $\Pi_X(z, \mathbf{q})$, being a one-loop integral involving mean-field quark propagators and thus not self-consistently determined. We shall come back to the issue of self-consistency in a separate work.

### 4.2. Phase shifts and the Levinson theorem for meson dissociation

Now we want to show that the phase (84) can be decomposed into two parts, corresponding to a structureless scattering continuum $\delta_c$ and a resonant (collective) contribution $\delta_R$ which under appropriate conditions represents a bound state contribution.

The following derivation holds whenever the polarization loop integral can be expressed in the form

$$\Pi_X(z, \mathbf{q}) = \Pi_{X,0} + \Pi_{X,2}(z, \mathbf{q}), \tag{91}$$

where $\Pi_{X,0}$ is a 4-momentum independent, real number, which can be a function of external thermodynamic variables. We will show that for this very general form the decomposition $\delta_X = \delta_{X,c} + \delta_{X,R}$ holds, whereby $\delta_{X,R}$ corresponds to a resonant mode which goes over to the real bound state at the Mott transition where the bound state energy meets the threshold of the continuum of scattering states. The latter are described by $\delta_{X,c}$, a structureless continuum background phase shift with a threshold to be directly identified from inspection of $\mathrm{Im}\,\Pi_X$ as given in Appendices A.3 and A.4. Here we generalize a result which has been derived for the pion and sigma channels before in [60] for the NJL model and in [22] for the Polyakov-loop extended NJL model.

The two-particle propagator $S_X$ in Eq. (85) can be given the form

$$\begin{aligned} S_X(z - \mu_X + \mathrm{i}\eta, \mathbf{q}) &= \frac{1}{G_X^{-1} - \Pi_{X,0} - \Pi_{X,2}(z - \mu_X + \mathrm{i}\eta, \mathbf{q})} \\ &= \frac{1}{\Pi_{X,2}(z - \mu_X + \mathrm{i}\eta, \mathbf{q})} \frac{1}{R_X(z^2, \mathbf{q}) - 1}, \end{aligned} \tag{92}$$

where the auxiliary function

$$R_X(z^2, \mathbf{q}) = \frac{1 - G_X \Pi_{X,0}}{G_X \Pi_{X,2}(z - \mu_X + \mathrm{i}\eta, \mathbf{q})} \tag{93}$$

has been introduced. Now it obviously holds

$$\ln S_X(z - \mu_X + \mathrm{i}\eta, \mathbf{q})^{-1} = \ln \Pi_{X,2}(z - \mu_X + \mathrm{i}\eta, \mathbf{q}) + \ln[R_X(z^2, \mathbf{q}) - 1], \tag{94}$$

so that with (84)

$$\delta_X(\omega, \mathbf{q}) = \delta_{X,c}(\omega, \mathbf{q}) + \delta_{X,R}(\omega, \mathbf{q}), \tag{95}$$

where

$$\delta_{X,c}(\omega, \mathbf{q}) = -\arctan\left(\frac{\mathrm{Im}\,\Pi_{X,2}(\omega - \mu_X + \mathrm{i}\eta, \mathbf{q})}{\mathrm{Re}\,\Pi_{X,2}(\omega - \mu_X + \mathrm{i}\eta, \mathbf{q})}\right), \tag{96}$$

$$\delta_{X,R}(\omega, \mathbf{q}) = \arctan\left(\frac{\mathrm{Im}\,R_X(\omega^2, \mathbf{q})}{1 - \mathrm{Re}\,R_X(\omega^2, \mathbf{q})}\right). \tag{97}$$

From this decomposition of the phase shift it becomes immediately obvious that $\delta_{X,R}(\omega, \mathbf{q})$ corresponds to the phase shift of a resonance at $\omega = \omega_X = \sqrt{\mathbf{q}^2 + m_X^2}$. The position of the resonance is found from the condition $\mathrm{Re}\,R_X(\omega_X^2) = 1$, where for brevity we drop here and in the following derivation the argument $\mathbf{q}$. At this energy it holds that $\delta_{X,R}(\omega \to \omega_X) \to \pi/2$ since $\tan \delta_{X,R}(\omega \to \omega_X) \to \infty$.

Performing a Taylor expansion at the resonance position for real $\omega$ one obtains

$$1 - \mathrm{Re}\, R_X(\omega^2) \approx \underbrace{1 - \mathrm{Re}\, R_X(\omega_X^2)}_{=0} - (\omega^2 - \omega_X^2)\mathrm{Re}\, \frac{\mathrm{d}R_X(z^2)}{\mathrm{d}z^2}\bigg|_{z=\omega_X}, \tag{98}$$

$$\mathrm{Im}\, R_X(\omega^2) \approx \mathrm{Im}\, R_X(\omega_X^2). \tag{99}$$

From this follows

$$\frac{1 - \mathrm{Re}\, R_X(\omega^2)}{\mathrm{Im}\, R_X(\omega^2)} \approx -(\omega^2 - \omega_X^2)\frac{\mathrm{Re}\, \frac{\mathrm{d}R_X(z^2)}{\mathrm{d}z^2}\Big|_{z=\omega_X}}{\mathrm{Im}\, R_X(\omega_X^2)}. \tag{100}$$

If we now define that

$$\omega_X \Gamma_X = -\frac{\mathrm{Im}\, R_X(\omega_X^2)}{\mathrm{Re}\, \frac{\mathrm{d}R_X(z^2)}{\mathrm{d}z^2}\Big|_{z=\omega_X}}, \tag{101}$$

the resonant phase shift becomes

$$\delta_{X,R}(\omega, \mathbf{q}) = \arctan\left(\frac{\omega_X \Gamma_X}{\omega^2 - \omega_X^2}\right), \tag{102}$$

which corresponds to the Breit–Wigner form for the spectral density in the Beth–Uhlenbeck EoS

$$\frac{\mathrm{d}\delta_{X,R}(\omega)}{\mathrm{d}\omega} = \frac{2\omega\omega_X\Gamma_X}{(\omega^2 - \omega_X^2)^2 + \omega_X^2\Gamma_X^2}. \tag{103}$$

This form goes over to the spectral density of a bound state when the width parameter $\Gamma_X \to 0$,

$$\lim_{\Gamma_X \to 0} \frac{\mathrm{d}\delta_{X,R}(\omega)}{\mathrm{d}\omega} = \pi\left[\delta(\omega - \omega_X) + \delta(\omega + \omega_X)\right], \tag{104}$$

with the Dirac $\delta$ distribution on the r.h.s.

The continuum contribution is defined along a cut on the real axis in the complex energy plane, i.e. for $\omega \geq \omega_{\mathrm{thr}}(\mathbf{q}) = \sqrt{\mathbf{q}^2 + 4m^2}$, where $\mathrm{Im}\, \Pi_2 \neq 0$. The value of the corresponding phase shift at threshold vanishes, $\delta_{X,c}(\omega_{\mathrm{thr}}) = 0$.

If the energy of the state $X$ is below that threshold, $\omega_X < \omega_{\mathrm{thr}}$, it is a real bound state with vanishing width ($\Gamma_X = 0$, infinite lifetime) and the resonant phase shift behaves as a step function which jumps by $\pi$ at $\omega = \omega_X$ and has therefore this value at the threshold, $\delta_{X,R}(\omega_{\mathrm{thr}}) = \pi$ for $T < T_{X,\mathrm{Mott}}$. In Fig. 1 we show the behavior of the threshold, the meson masses and the pion width in sections through the phase diagram in the $T$, $\mu$-plane, for $\mathbf{q} = 0$. Note that the sharp onset of the pion width at the Mott temperatures is an artifact of the present approximation which neglects $\pi$–$\pi$ scattering and treats quarks in the mean field approximation only, where they are on-shell quasiparticles with zero width.

The parameters employed are a bare quark mass $m_0 = 5.5$ MeV, a three-momentum cutoff $\Lambda = 639$ MeV and a scalar coupling constant $G_S\Lambda^2 = 2.134$. We consider two alternative values for the diquark coupling constant: a strong coupling $G_D = G_S$, and a moderate coupling $G_D = 3/4\, G_S$. The latter is motivated by the ratio between scalar diquark and scalar meson interaction channels arising from a Fierz transformation of the (massive) vector boson exchange interaction model (see, e.g., Eq. (A.20) in the Appendix A of Ref. [38]). With the above parameters one finds in vacuum a constituent quark mass of 319 MeV, a pion mass of 138 MeV and pion decay constant $f_\pi = 92.4$ MeV. The vacuum mass of the $\sigma$-meson is 644 MeV, which is thus slightly unbound. The scalar diquark is bound (pion-like) for the strong diquark coupling and slightly unbound (sigma-like) for the Fierz value of the coupling. Masses and widths of mesons and diquarks are determined from the solution of the corresponding Bethe–Salpeter equations, *i.e.,* from the (complex) poles of their two-particle propagators, see Sections 2.2 and 3.

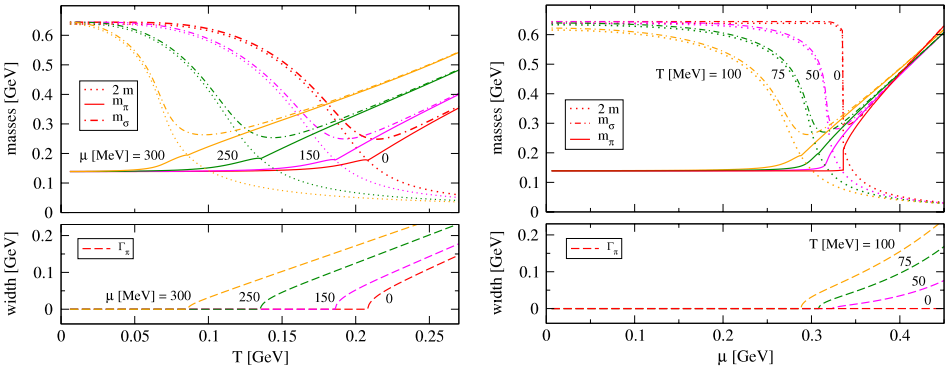


**Fig. 1.** (Color online) Two-particle spectrum in the scalar–pseudoscalar meson channels at rest in the medium ($\mathbf{q} = 0$). Left panel: Behavior of the thresholds for the quark–antiquark continuum $2m$ (dotted lines), meson masses ($m_\sigma$ —dash–dotted lines, $m_\pi$ —solid lines) and pion width $\Gamma_\pi$ (dashed lines) as functions of $T$ for different values of the chemical potential $\mu$. Right panel: Same as the left panel but as functions of $\mu$ for different temperatures $T$.

The Mott transition, when the bound state merges the continuum, can be detected also from the behavior of the resonant phase shift which will be subject to the same threshold as the continuum and vanishes at the continuum edge, $\delta_{X,R}(\omega_{\rm thr}) = 0$ for $T > T_{X,\rm Mott}$. This is a manifestation of Levinson's theorem II which can be formulated as

$$\int_0^\infty {\rm d}\omega \frac{1}{\pi}\frac{{\rm d}\delta_X(\omega;T)}{{\rm d}\omega} = 0 = \underbrace{\int_0^{\omega_{\rm thr}(T)} {\rm d}\omega \frac{1}{\pi}\frac{{\rm d}\delta_X(\omega;T)}{{\rm d}\omega}}_{n_{B,X}(T)} + \underbrace{\frac{1}{\pi}\int_{\omega_{\rm thr}(T)}^\infty {\rm d}\omega \frac{{\rm d}\delta_X(\omega;T)}{{\rm d}\omega}}_{\frac{1}{\pi}[\delta_X(\infty;T)-\delta_X(\omega_{\rm thr};T)]}, \tag{105}$$

at any given temperature $T$. Since under very general conditions [56] holds $\delta_X(\infty;T) = 0$ for any temperature it follows that $\delta_X(\omega_{\rm thr};T) = \pi n_{B,X}(T)$, *i.e.,* that decrementing the number of bound states in the channel $X$ at the corresponding Mott temperature $T_{X,\rm Mott}$ has to be accompanied by a jump by $\pi$ of the phase shift at threshold [57]. This behavior is illustrated in Fig. 2, see also Refs. [22,24].

### 4.3. Thermodynamics of Mott dissociation

In this subsection, we demonstrate first for the case of the pion as the lightest meson and then for the scalar diquark, how the Mott dissociation of the bound state leads to a reduction of the correlation contribution to the thermodynamical potential. All thermodynamic relations can be consistently derived from the thermodynamic potential which for a homogeneous system is directly given by the pressure. For the following numerical investigation we focus on $X = \pi, \delta_A, \delta_A^*$.

#### 4.3.1. The case of the lightest meson

In order to discuss the pressure for pion correlations in quark matter we start from the expression (90). We respect that $\mu_\pi = 0$ so that the GBU EoS for the pion pressure takes the form

$$p_\pi(T) = -d_\pi T \int \frac{{\rm d}^3q}{(2\pi)^3}\int_0^\infty \frac{{\rm d}\omega}{\pi}\,\ln\left(1-{\rm e}^{-\omega/T}\right)\frac{{\rm d}\delta_\pi(\omega,\mathbf{q})}{{\rm d}\omega}. \tag{106}$$

This equation encodes the in-medium modification of the pionic correlations including their Mott dissociation in the behavior of the phase shift $\delta_\pi(\omega,\mathbf{q})$ which is defined by Eqs. (95)–(97) via the polarization function examined in detail in Appendix. For a recent numerical evaluation of the pion and sigma meson thermodynamics within the PNJL model, see [23].

We want to give here a qualitative discussion of the physics content of the GBU EoS (106) by considering the phase shifts for pions at rest in the medium, as shown in Fig. 2, and suggesting their

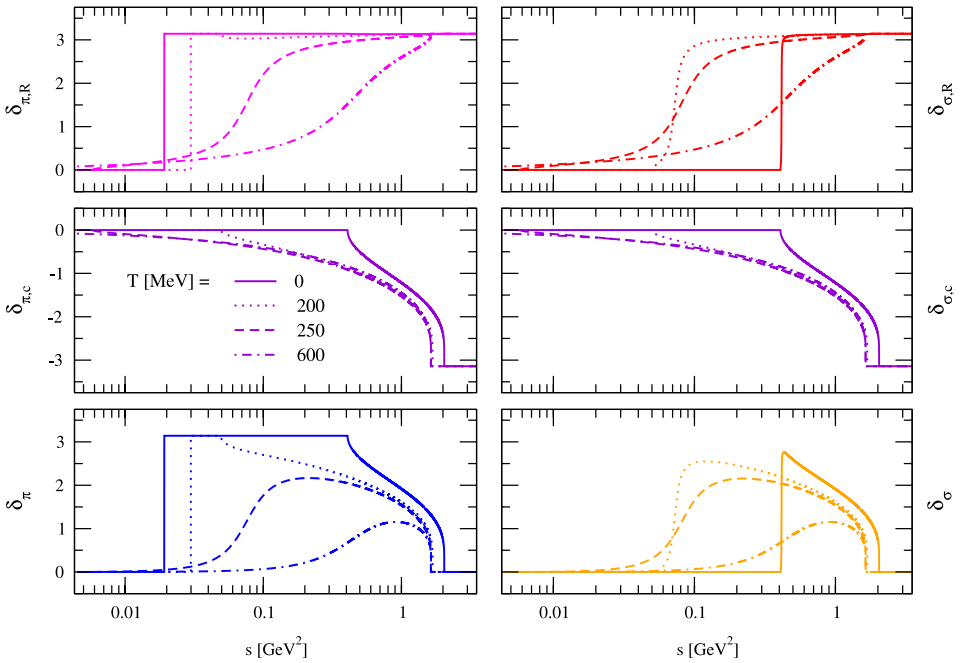


**Fig. 2.** Phase shifts for pion (left panels) and sigma meson (right panels) channels at rest ($\mathbf{q} = 0$) as functions of the squared mass variable $s = \omega^2$ for different temperatures, below ($T = 0$, 200 MeV) and above ($T = 250$, 600 MeV) the Mott-transition. The upper panels show the resonant phase shifts which together with the continuum phase shifts shown in the middle panels add up to the total phase shifts of the bottom panels.

approximate boost invariance depending on $\omega$ and $\mathbf{q}$ only via the Mandelstam variable $s = \omega^2 - q^2$ in the form $\delta_\pi(\omega, \mathbf{q} = 0) = \delta_\pi(\sqrt{s}, \mathbf{q} = 0) \equiv \delta_\pi(s; T)$. Then, the GBU EoS for the pionic pressure can be given the suggestive form[1]

$$p_\pi(T) = \int_0^\infty \mathrm{d}s\, D_\pi(s; T)\, p_\pi(T, s), \tag{107}$$

where

$$p_\pi(T, s) = -d_\pi T \int \frac{\mathrm{d}^3 q}{(2\pi)^3} \ln\left(1 - \mathrm{e}^{-\sqrt{q^2+s}/T}\right) \tag{108}$$

is the pressure of a relativistic Bose gas of pions with a fictitious mass $\sqrt{s}$. The distribution of these masses to be integrated over for obtaining the total pressure is given by the density of states

$$D_\pi(s; T) = \frac{1}{\pi} \frac{\mathrm{d}\delta_\pi(s; T)}{\mathrm{d}s}. \tag{109}$$

Exploiting the analytic decomposition of the total phase shift (95) into a continuum and a resonant contribution, $\delta_\pi = \delta_{\pi,c} + \delta_{\pi,R}$, we can separate the pion pressure into a negative continuum contribution and a resonance contribution, $p_\pi(T) = p_{\pi,c}(T) + p_{\pi,R}(T)$, where for the latter we can

[1] Formally, when substituting the $\omega$-integral in (106) for a $s$-integral, the lower limit $\omega_{\min} = 0$ corresponds to $s_{\min} = -q^2$. Because of the interpretation of the variable $s$ as a squared meson mass, we restrict the range of the $s$-integration to all nonnegative values.

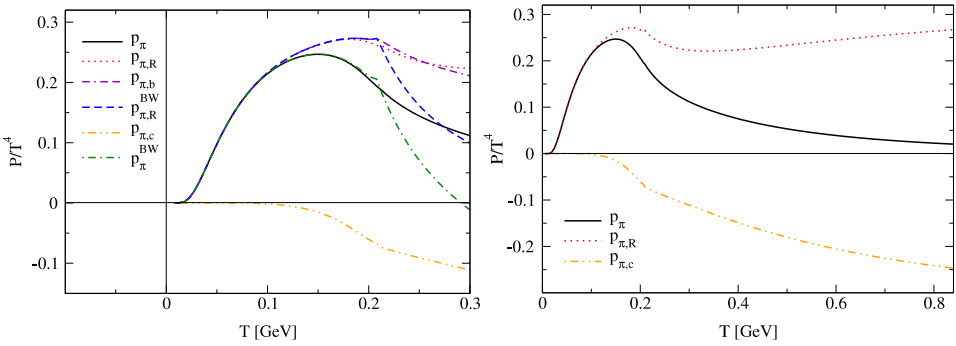


**Fig. 3.** Right panel: Pionic contribution to the pressure, Eq. (107), as a function of the temperature $T$ for chemical potential $\mu = 0$ (solid line) and its decomposition into resonant (dotted line) and continuum (dash–double-dotted line) scattering contributions according to the decomposition of the phase shift in the density of states Eq. (109). Left panel: Closeup of the right panel in the temperature region of the pion Mott transition at $T_{\pi,\mathrm{Mott}} = 208$ MeV and comparison to different approximations for the resonance contribution: The dashed line represents the Breit–Wigner approximation (110) for the resonance contribution and shows the effect of the resonance broadening compared to the pion bound state approximation (111), with a $T$-dependent mass but without broadening (dot–double-dashed line). The dash–dotted line shows the total pion pressure when for the resonance contribution the Breit–Wigner approximation is used. Note that the effect of the continuum pressure sets in already before the Mott transition temperature is reached.

make use of the Breit–Wigner approximation (103)

$$D^{BW}_{\pi,R}(s;T) = \frac{1}{\pi}\frac{\Gamma_\pi m_\pi}{(s-m_\pi^2)^2+\Gamma_\pi^2 m_\pi^2}, \tag{110}$$

for which holds that

$$\lim_{\Gamma_\pi\to 0} D^{BW}_{\pi,R}(s;T) = D_{\pi,\mathrm{bound}} = \delta(s-m_\pi^2). \tag{111}$$

In the limit of vanishing width $\Gamma_\pi \to 0$ the resonance goes over to an ideal bound state with infinite lifetime. Then the $s$-integration in (107) can be analytically performed and yields the ideal pion gas form $p_\pi(T, m_\pi^2)$, here with a temperature dependent mass $m_\pi = m_\pi(T)$. Since the pion mass is rising with temperature (see Fig. 1), in particular for $T > T_{\chi,\mathrm{Mott}}$, the corresponding pressure shows a slight drop (dot–double-dashed line in Fig. 3).

Taking into account additionally the rapidly growing pion width $\Gamma_\pi(T)$ with a sharp onset at $T = T_{\chi,\mathrm{Mott}}$ (see Fig. 1), the pion pressure is reduced stronger above the Mott temperature (dashed line in Fig. 3). In these approximations, the role of the continuum has been neglected. The pressure of the continuum states $p_{\pi,c}(T)$ on the other hand is obtained when the resonance contribution (dotted line in Fig. 3) to the density of states is neglected, *i.e.*,

$$D_\pi(s;T) = D_{\pi,c}(s;T) = \frac{1}{\pi}\frac{\mathrm{d}\delta_{\pi,c}(s;T)}{\mathrm{d}s} \tag{112}$$

is used in Eq. (107). The result is shown as the dash–double-dotted line in Fig. 3; its contribution is negative and sets in already for $T < T_{\chi,\mathrm{Mott}}$. The total pion pressure (solid line in Fig. 3) with contributions from both resonant and continuum scattering shows a typical behavior with increasing temperature: first a rise towards the Stefan–Boltzmann limit which, however, is never reached because the lowering of the continuum edge due to the chiral phase transition induces a reduction of the meson gas pressure already before the Mott temperature is reached. Second, above the Mott temperature, the growing pion width leads to a stronger reduction of the pressure with a rather sharp onset of this effect. The resulting pattern appears like a "shark fin".

### *4.3.2. Mott dissociation of diquarks*

The introduction of diquark fields is a prerequisite for the description of baryons as quark–diquark bound states in a chiral quark model. Thereby the diquark appears not necessarily as a bound state.

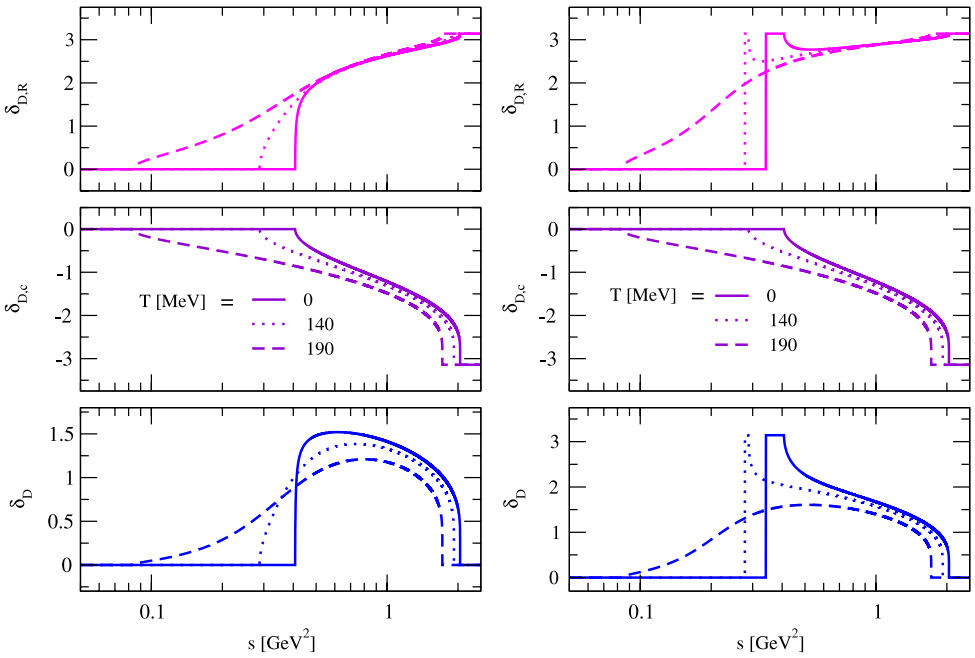


**Fig. 4.** Phase shifts for the scalar diquark channel with $G_D = 3/4\,G_S$ (left panels) and $G_D = G_S$ (right panels) at rest ($\mathbf{q} = 0$) as functions of the squared mass variable $s = \omega^2$ for different temperatures $T = 0$, 140, 190 MeV. The upper panels show the resonant phase shifts which together with the continuum phase shifts shown in the middle panels add up to the total phase shifts of the bottom panels. Comparison to Fig. 2 shows that for moderate coupling (left panels) the diquark behaves "sigma-like", since it is unbound for all temperatures. For strong coupling (right panels) the diquark behaves "pion-like", since it is a bound state for low temperatures and exhibits a Mott transition at $T \approx 140$ MeV where the phase shift at the continuum threshold $s_{\rm thr} = 4m^2$ jumps from the value $\pi$ to zero in accordance with the Levinson theorem (105).

Actually, in particular in QCD DSE approaches the diquark is unbound while the baryon is a bound state, like in a Borromean three-particle state.

Having developed in the present work the theoretical basis for the description of the thermodynamics of mesons and diquarks in hot and dense quark matter including a Mott dissociation transition, we want to discuss now after the pion also the diquark case. To that end we focus here on the normal quark matter phase and evaluate the diquark phase shifts for vanishing chemical potential at finite temperatures which encode the analytic properties of the diquark propagator. The results are shown in Fig. 4 for two cases of the diquark coupling strength: the moderate one (left panels) which corresponds to the Fierz value $G_D = 3/4\,G_S$ and the strong coupling case (right panels) with $G_D = G_S$. In the latter case the diquark is a bound state at zero temperature and its phase shift behaves similar to that of the pion in Fig. 2 which exhibits a Mott transition to an unbound resonance in the continuum at a certain temperature. For our parametrization this happens at $T_{D,\rm Mott} \approx 140$ MeV. For the moderate coupling case, the diquark phase shift is shown in the left panels of Fig. 2 and behaves similar to the sigma meson: it is already an unbound resonant scattering state in the vacuum at $T = 0$ and becomes even less correlated when the temperature is increased.

The diquark contribution to the thermodynamics is evaluated according to the Beth–Uhlenbeck formula (90) for the pressure, where, as in the pion case, the "no sea" approximation is applied, *i.e.,* the contribution of the zero-point energy in (89) is removed. The result is shown in Fig. 5 for the Fierz coupling case (left panel) which exhibits an almost complete compensation between the contributions of the diquarks resonance and the scattering continuum so that the resulting pressure (solid line) in the diquark channel is much smaller than that of the pion channel albeit with a similar shape. The comparison with the strong coupling case (right panel) shows that the continuum background

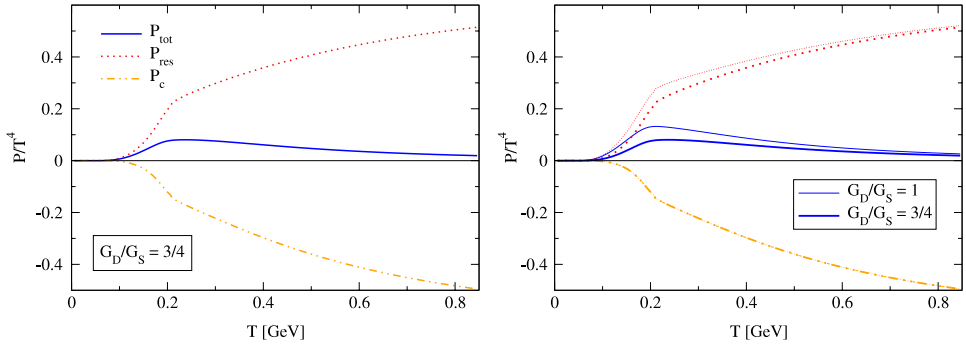


**Fig. 5.** Pressure for the scalar diquark (solid line) with its resonant (dotted line) and continuum (dash–double-dotted line) components as functions of temperature. Bold lines are for the case of the moderate (Fierz) coupling $G_D/G_S = 3/4$ (left and right panel) while thin lines are for the strong coupling case $G_D/G_S = 1$ (right panel).

pressure is unaffected while the resonance contribution with the diquark Mott transition shows a moderate overall increase.

### *4.4. Further developments*

A key lesson from this investigation into the GBU EoS for the two-particle correlations in the pion and diquark channels in hot quark matter is that accounting for the broadening of hadronic states due to the Mott transition alone it is not sufficient and would violate the Levinson theorem [22, 24]. One has to account for the scattering state continuum which influences the thermodynamics as soon as the thermal energy is of the order of the dissociation threshold, the gap between bound and continuum states of the spectrum. This appears to be an important modification of the so-called "chemical" picture where hadron species form a statistical ensemble of quasiparticles which goes beyond attributing to these hadronic resonances a finite lifetime (width). The more elaborate "physical" picture requires to account for a scattering state continuum which in a systematic way is given by a virial expansion and as such appears in the GBU EoS. For a discussion of the cluster virial expansion in nuclear matter see, *e.g.*, [61].

For dense hadronic matter, where hadrons play the role of clusters, a similar approach is still to be developed. We suggest that this could be done along the lines of the GBU approach given here. However, the problem one is facing when one wants to build such an approach on an NJL-type model is the lack of confinement. In the NJL model used here, just the pions are bound states in the vacuum while the sigma meson is already an unbound resonance, decaying to quarks. In the flavor SU(3) extension of the NJL model, it is just the pseudoscalar meson octet which is bound while the other channels important for the phenomenology (vector, scalar and axial vector mesons) are unbound.

While a solution to this severe problem has still to be worked out, there are simple extensions of the NJL model which can be used to remove unphysical quark decay thresholds but still keep the microscopic description of the hadron Mott effect sufficiently simple. One of such extensions mimics confining interactions by suppressing long wavelength modes in quark propagation by applying a low-momentum cutoff to quark loop integrals. Moreover, since confinement and chiral symmetry breaking shall be related, this cutoff has been fixed to the dynamically generated quark mass gap which vanishes upon chiral symmetry restoration. For details, see [24] and references therein. In this work it has been shown how this infrared cutoff increases the threshold for quark–antiquark scattering states and thus makes the $\sigma$-meson a bound state in the chiral symmetry broken phase for low temperatures. It could also be demonstrated in [24] within this NJL model generalized by a low-momentum cutoff, that the shape of the phase shifts and their temperature dependence for the $\sigma$-meson becomes similar to that of the pion, where the transition from a bound state to a resonance in the continuum can be recognized in accordance with the Levinson theorem. Summarizing this section, we would like to point out that the NJL model and its modifications provide a useful tool for a field

theoretic formulation of the physics of the Mott dissociation of hadrons as quark bound states in hot, dense quark matter or, conversely, of the hadronization of quark correlations in an expanding and cooling QGP.

## 5. Conclusions

In this work, we have presented a general approach to the discussion of two-particle correlations in quark matter within a field theoretical chiral quark model of the NJL type. By restricting the expansion of the fermion determinant of the bosonized partition function to the Gaussian approximation, the path integral over the meson and diquark fluctuations can be performed and a closed expression is obtained in the form of the determinant of a generalized matrix propagator for two-particle states (meson and diquark fields). The diagonalization of this matrix defines the mode spectrum of the model. A detailed discussion of limiting cases (chiral limit, zero momentum limit) is performed and analytic expressions are given.

Nambu–Goldstone (NG) modes in the 2SC phase are considered and the finite $T$ extension of the work by Ebert and collaborators [42] is provided here for the first time. It is demonstrated that in the 2SC phase there are only 3 instead of 5 massless NG modes, in accordance with the Nielsen–Chadha theorem.

We have discussed the interplay between bound and scattering states in the medium, in particular at the Mott transition where the bound state transforms to a resonance in the continuum. This transition is reflected in a vanishing of the binding energy as well as a jump by $\pi$ of the phase shift at threshold in accordance with the Levinson theorem.

The thermodynamic potential is given the form of a generalized Beth–Uhlenbeck equation where special emphasis is on the discussion of the role of the continuum contributions as well as of the resonant two-particle correlations as expressed in terms of the in-medium scattering phase shifts. It is shown that accounting for the spectral broadening of hadrons alone is insufficient to account for the Mott dissociation. Only together with the continuum states can be guaranteed that the result for the pressure is in accordance with the in-medium Levinson theorem.

The in-medium phase shifts for mesonic and diquark correlation channels as evaluated in this work within a NJL model description of low energy QCD contain spectral information which may be exploited to study mesonic and diquark correlation functions at finite temperature, around the chiral restoration. It will be very interesting to investigate how the Mott transition for mesons manifests itself in these functions for which also ab initio calculations using lattice QCD simulations exist. We plan to extend our work in this direction and to provide guidance from this low-energy QCD model for the interpretation of those lattice QCD data.

An outlook is given to the further development of the approach towards a description of meson–baryon matter on the basis of chiral quark models of the NJL type which shall be detailed in subsequent work.

## Acknowledgments

We acknowledge R. Anglani for his collaboration in an early stage of this work and T. Brauner for discussions and his critical reading of the manuscript. This work was supported by the Deutsche Forschungsgemeinschaft (DFG) under contract BU 2406/1-1 and by the Polish National Science Centre within the "Maestro" programme under grant no. UMO-2011/02/A/ST2/00306. The work of D.B. was supported in part by the Polish Ministry of Science and Higher Education (MNiSW) under grant no. 1009/S/IFT/14. G.R. and D.B. are grateful to the Erasmus programme and partnership between Universities of Rostock and Wroclaw which supported mutual visits.

## Appendix. Meson and diquark polarization functions

In this appendix we give explicit expressions for the elements of the polarization matrix $\Pi$ defined in Eq. (62). We thereby neglect the vector fields $\omega_\mu$. Moreover, since the three isospin components of

the pion are degenerate and do not mix with each other or any other mode, we only list one generic component here for simplicity.

### A.1. 2SC phase

In the 2SC phase, the polarization matrix has the structure

$$\Pi = \begin{pmatrix} \Pi_{\pi\pi} & 0 & 0 & 0 & 0 & 0 & 0 & 0 \\ 0 & \Pi_{\sigma\sigma} & \Pi_{\sigma\delta_2} & \Pi_{\sigma\delta_2^*} & 0 & 0 & 0 & 0 \\ 0 & \Pi_{\delta_2^*\sigma} & \Pi_{\delta_2^*\delta_2} & \Pi_{\delta_2^*\delta_2^*} & 0 & 0 & 0 & 0 \\ 0 & \Pi_{\delta_2\sigma} & \Pi_{\delta_2\delta_2} & \Pi_{\delta_2\delta_2^*} & 0 & 0 & 0 & 0 \\ 0 & 0 & 0 & 0 & \Pi_{\delta_5^*\delta_5} & 0 & 0 & 0 \\ 0 & 0 & 0 & 0 & 0 & \Pi_{\delta_5\delta_5^*} & 0 & 0 \\ 0 & 0 & 0 & 0 & 0 & 0 & \Pi_{\delta_7^*\delta_7} & 0 \\ 0 & 0 & 0 & 0 & 0 & 0 & 0 & \Pi_{\delta_7\delta_7^*} \end{pmatrix}. \tag{A.1}$$

Each matrix element depends on an external three-momentum $\mathbf{q}$ and an external bosonic Matsubara frequency $\mathrm{i}z_n$, which after analytic continuation becomes the complex variable $z$. Labeling the fields in the vector (61) by $i = \vec{\pi}^T, \sigma, \delta_2^*, \delta_2, \delta_5^*, \delta_5, \delta_7^*, \delta_7$ and $j = \vec{\pi}, \sigma, \delta_2, \delta_2^*, \delta_5, \delta_5^*, \delta_7, \delta_7^*$, we have

$$\Pi_{ij} \equiv \Pi_{ij}(\mathrm{i}z_n, \mathbf{q}) \equiv \Pi_{ij}(z, \mathbf{q}). \tag{A.2}$$

The explicit expressions as listed below also contain an internal momentum $\mathbf{p}$ which is integrated over. It is then convenient to define a third momentum $\mathbf{k} = \mathbf{p} - \mathbf{q}$.

The individual elements are as follows

$$\begin{aligned} \Pi_{\pi\pi} &= \frac{1}{2} N_f \int \frac{\mathrm{d}^3 p}{(2\pi)^3} \sum_{s_p, s_k} \mathcal{T}_-^+(s_p, s_k) \\ &\quad \times \left\{ \frac{n(s_p \xi_{\mathbf{p}}^{s_p}) - n(s_k \xi_{\mathbf{k}}^{s_k})}{z - s_k \xi_{\mathbf{k}}^{s_k} + s_p \xi_{\mathbf{p}}^{s_p}} - \frac{n(s_p \xi_{\mathbf{p}}^{s_p}) - n(s_k \xi_{\mathbf{k}}^{s_k})}{z + s_k \xi_{\mathbf{k}}^{s_k} - s_p \xi_{\mathbf{p}}^{s_p}} \right. \\ &\quad \left. + \sum_{t_p, t_k} F(s_p, s_k; t_p, t_k) \left( t_p t_k E_{\mathbf{p}}^{s_p} E_{\mathbf{k}}^{s_k} + s_p s_k \xi_{\mathbf{p}}^{s_p} \xi_{\mathbf{k}}^{s_k} - |\Delta_{\mathrm{MF}}|^2 \right) \right\} \end{aligned} \tag{A.3}$$

$$\Pi_{\delta_2 \delta_2} = \frac{1}{4} (\Delta_{\mathrm{MF}}^*)^2 N_f \int \frac{\mathrm{d}^3 p}{(2\pi)^3} \sum_{\substack{s_p, t_p \\ s_k, t_k}} \mathcal{T}_+^+(s_p, s_k) F(s_p, s_k; t_p, t_k) \tag{A.4}$$

$$\begin{aligned} \Pi_{\delta_2^* \delta_2} &= \frac{1}{4} N_f \int \frac{\mathrm{d}^3 p}{(2\pi)^3} \sum_{\substack{s_p, t_p \\ s_k, t_k}} \mathcal{T}_+^+(s_p, s_k) F(s_p, s_k; t_p, t_k) \\ &\quad \times (t_p E_{\mathbf{p}}^{s_p} + s_p \xi_{\mathbf{p}}^{s_p})(t_k E_{\mathbf{k}}^{s_k} - s_k \xi_{\mathbf{k}}^{s_k}) \end{aligned} \tag{A.5}$$

$$\begin{aligned} \Pi_{\sigma \delta_2} &= \frac{1}{4} m \Delta_{\mathrm{MF}}^* N_f \int \frac{\mathrm{d}^3 p}{(2\pi)^3} \sum_{\substack{s_p, t_p \\ s_k, t_k}} \left( \frac{s_p}{E_{\mathbf{p}}} + \frac{s_k}{E_{\mathbf{k}}} \right) F(s_p, s_k; t_p, t_k) \\ &\quad \times \left[ \left( t_p E_{\mathbf{p}}^{s_p} - t_k E_{\mathbf{k}}^{s_k} \right) + \left( s_p \xi_{\mathbf{p}}^{s_p} + s_k \xi_{\mathbf{k}}^{s_k} \right) \right] \end{aligned} \tag{A.6}$$

$$\begin{aligned} \Pi_{\delta_5^* \delta_5} &= \frac{1}{2} N_f \int \frac{\mathrm{d}^3 p}{(2\pi)^3} \sum_{\substack{s_p, t_p \\ s_k, t_k}} \mathcal{T}_+^+(s_p, s_k) \left\{ \frac{E_{\mathbf{p}}^{s_p} - s_p t_p \xi_{\mathbf{p}}^{s_p}}{E_{\mathbf{p}}^{s_p}} \frac{n(s_k \xi_{\mathbf{k}}^{s_k}) - n(t_p E_{\mathbf{p}}^{s_p})}{z - t_p E_{\mathbf{p}}^{s_p} + s_k \xi_{\mathbf{k}}^{s_k}} \right. \\ &\quad \left. + \frac{E_{\mathbf{k}}^{s_k} - s_k t_k \xi_{\mathbf{k}}^{s_k}}{E_{\mathbf{k}}^{s_k}} \frac{n(s_p \xi_{\mathbf{p}}^{s_p}) - n(t_k E_{\mathbf{k}}^{s_k})}{z - t_k E_{\mathbf{k}}^{s_k} + s_p \xi_{\mathbf{p}}^{s_p}} \right\} \end{aligned} \tag{A.7}$$

and the remaining elements are recast by the replacements

$$\Pi_{\sigma\sigma} = \Pi_{\pi\pi}\left(\mathcal{T}_-^+ \to \mathcal{T}_-^-\right) \tag{A.8}$$

$$\Pi_{\delta_2^*\delta_2^*} = \Pi_{\delta_2\delta_2}\left((\Delta_{\rm MF}^*)^2 \to \Delta_{\rm MF}^2\right) \tag{A.9}$$

$$\Pi_{\delta_2\delta_2^*} = \Pi_{\delta_2^*\delta_2}\left(z \to -z, \mathbf{p} \leftrightarrow \mathbf{k}\right) \tag{A.10}$$

$$\Pi_{\sigma\delta_2^*} = \Pi_{\sigma\delta_2}\left(\Delta_{\rm MF}^* \to \Delta_{\rm MF}, \mathbf{p} \leftrightarrow \mathbf{k}\right) \tag{A.11}$$

$$\Pi_{\delta_2^*\sigma} = \Pi_{\sigma\delta_2}\left(\Delta_{\rm MF}^* \to \Delta_{\rm MF}, z \to -z\right) \tag{A.12}$$

$$\Pi_{\delta_2\sigma} = \Pi_{\sigma\delta_2^*}\left(\Delta_{\rm MF} \to \Delta_{\rm MF}^*, z \to -z\right) \tag{A.13}$$

$$\Pi_{\delta_5\delta_5^*} = \Pi_{\delta_5^*\delta_5}\left(z \to -z, \mathbf{p} \leftrightarrow \mathbf{k}\right) \tag{A.14}$$

$$\Pi_{\delta_7\delta_7^*} = \Pi_{\delta_5\delta_5^*} \tag{A.15}$$

$$\Pi_{\delta_7^*\delta_7} = \Pi_{\delta_5^*\delta_5}. \tag{A.16}$$

Here $s_p, s_k; t_p, t_k = \pm 1$ are sign operators, $E_{\mathbf{p}}$, $E_{\mathbf{p}}^{\pm}$, and $\xi_{\mathbf{p}}^{\pm}$ are the single-quark dispersion relations, given in Section 2.1, and $n(x)$ denotes again the Fermi distribution function. Moreover, we have defined

$$F(s_p, s_k; t_p, t_k) = \frac{t_p t_k}{E_{\mathbf{p}}^{s_p} E_{\mathbf{k}}^{s_k}} \frac{n(t_p E_{\mathbf{p}}^{s_p}) - n(t_k E_{\mathbf{k}}^{s_k})}{z - t_k E_{\mathbf{k}}^{s_k} + t_p E_{\mathbf{p}}^{s_p}}, \tag{A.17}$$

and the kinematic pre-factors

$$\mathcal{T}_{\mp}^{\pm}(s, s') = 1 \mp s s' \frac{\mathbf{p}\cdot\mathbf{k} \pm m^2}{E_{\mathbf{p}} E_{\mathbf{k}}}. \tag{A.18}$$

### A.2. Correlations at rest

The expressions for the polarization functions get strongly simplified for correlations at rest, $\mathbf{q} = 0$. We then have $\mathbf{p} = \mathbf{k}$, which then puts restrictions on the summation over $s_p$ and $s_k$ via $\mathcal{T}_{\mp}^{\pm}$ and at last we can carry out the summations over $t_p$, $t_k$. This then leaves us with only one sign operator, which is then associated with particle $(-)$ and anti-particle $(+)$ contributions. We find

$$\Pi_{\pi\pi}(z, \mathbf{0}) = -8 I_\pi(z), \tag{A.19}$$

$$\Pi_{\sigma\sigma}(z, \mathbf{0}) = -8 I_\sigma(z) - 16 m^2 |\Delta_{\rm MF}|^2 I_4(z), \tag{A.20}$$

$$\Pi_{\delta_2^*\delta_2}(z, \mathbf{0}) = 2 I_\Delta + 4 z I_1(z) + (4|\Delta_{\rm MF}|^2 - 2z^2) I_0(z), \tag{A.21}$$

$$\Pi_{\delta_2\delta_2}(z, \mathbf{0}) = 4\Delta_{\rm MF}^2 I_0(z), \tag{A.22}$$

$$\Pi_{\sigma\delta_2}(z, \mathbf{0}) = -4 m \Delta_{\rm MF}(z I_2(z) + 2 I_3(z)), \tag{A.23}$$

$$\Pi_{\delta_5^*\delta_5}(z, \mathbf{0}) = I_\Delta + 2 z I_7(z) - (|\Delta_{\rm MF}|^2 - z^2) I_5(z), \tag{A.24}$$

and the remaining elements can be found by applying the symmetry relations Eqs. (A.9)–(A.16). The constant $I_\Delta$ and the functions $I_i(z)$ are defined as follows:

$$I_\Delta = I_\Delta^+ + I_\Delta^-, \qquad I_0 = I_0^+ + I_0^-, \tag{A.25}$$

$$I_1 = I_1^+ - I_1^-, \qquad I_2 = I_2^+ + I_2^-, \tag{A.26}$$

$$I_3 = I_3^+ + I_3^-, \qquad I_4 = I_4^+ + I_4^-, \tag{A.27}$$

$$I_5 = I_5^+ + I_5^-, \qquad I_7 = I_7^+ - I_7^-, \tag{A.28}$$

where the individual terms are

$$I_{\Delta}^{\pm} \equiv \int \frac{\mathrm{d}^3p}{(2\pi)^3}\left[1-2n(E_{\mathbf{p}}^{\pm})\right]\frac{1}{E_{\mathbf{p}}^{\pm}}, \qquad I_0^{\pm}(z) \equiv \int \frac{\mathrm{d}^3p}{(2\pi)^3}\frac{1}{E_{\mathbf{p}}^{\pm}}F_{\mathbf{p}}^{\pm}(z), \tag{A.29}$$

$$I_1^{\pm}(z) \equiv \int \frac{\mathrm{d}^3p}{(2\pi)^3}\frac{\xi_{\mathbf{p}}^{\pm}}{E_{\mathbf{p}}^{\pm}}F_{\mathbf{p}}^{\pm}(z), \qquad I_2^{\pm}(z) \equiv \int \frac{\mathrm{d}^3p}{(2\pi)^3}\frac{1}{E_{\mathbf{p}}}\frac{1}{E_{\mathbf{p}}^{\pm}}F_{\mathbf{p}}^{\pm}(z), \tag{A.30}$$

$$I_3^{\pm}(z) \equiv \int \frac{\mathrm{d}^3p}{(2\pi)^3}\frac{1}{E_{\mathbf{p}}}\frac{\xi_{\mathbf{p}}^{\pm}}{E_{\mathbf{p}}^{\pm}}F_{\mathbf{p}}^{\pm}(z), \qquad I_4^{\pm}(z) \equiv \int \frac{\mathrm{d}^3p}{(2\pi)^3}\frac{1}{E_{\mathbf{p}}^2}\frac{1}{E_{\mathbf{p}}^{\pm}}F_{\mathbf{p}}^{\pm}(z), \tag{A.31}$$

$$I_5^{\pm}(z) \equiv \int \frac{\mathrm{d}^3p}{(2\pi)^3}\frac{1-2n(E_{\mathbf{p}}^{\pm})}{E_{\mathbf{p}}^{\pm}(z^2 \pm z\xi_{\mathbf{p}}^{\pm} - |\Delta_{\mathrm{MF}}|^2)}, \qquad I_7^{\pm}(z) \equiv \int \frac{\mathrm{d}^3p}{(2\pi)^3}\frac{1-2n(\xi_{\mathbf{p}}^{\pm})}{z^2 \pm z\xi_{\mathbf{p}}^{\pm} - |\Delta_{\mathrm{MF}}|^2} \tag{A.32}$$

and the remaining integral for the mesons is given by

$$\begin{aligned} I_{\pi}(z) \equiv \int \frac{\mathrm{d}^3p}{(2\pi)^3}\Bigg\{ & \left[1-n(\xi_{\mathbf{p}}^{+})-n(\xi_{\mathbf{p}}^{-})\right]\frac{2E_{\mathbf{p}}}{z^2-4E_{\mathbf{p}}^2} \\ & + \frac{E_{\mathbf{p}}^{+}E_{\mathbf{p}}^{-}-\xi_{\mathbf{p}}^{+}\xi_{\mathbf{p}}^{-}-|\Delta_{\mathrm{MF}}|^2}{E_{\mathbf{p}}^{+}E_{\mathbf{p}}^{-}}\left[n(E_{\mathbf{p}}^{-})-n(E_{\mathbf{p}}^{+})\right]\frac{E_{\mathbf{p}}^{+}-E_{\mathbf{p}}^{-}}{z^2-\left(E_{\mathbf{p}}^{+}-E_{\mathbf{p}}^{-}\right)^2} \\ & + \frac{E_{\mathbf{p}}^{+}E_{\mathbf{p}}^{-}+\xi_{\mathbf{p}}^{+}\xi_{\mathbf{p}}^{-}+|\Delta_{\mathrm{MF}}|^2}{E_{\mathbf{p}}^{+}E_{\mathbf{p}}^{-}}\left[1-n(E_{\mathbf{p}}^{+})-n(E_{\mathbf{p}}^{-})\right]\frac{E_{\mathbf{p}}^{+}+E_{\mathbf{p}}^{-}}{z^2-\left(E_{\mathbf{p}}^{+}+E_{\mathbf{p}}^{-}\right)^2}\Bigg\}. \end{aligned} \tag{A.33}$$

The integral $I_{\sigma}(z)$ differs from $I_{\pi}(z)$ only by an additional overall factor $\mathbf{p}^2/E_{\mathbf{p}}^2$ in the integrand.

In the normal phase, for $\Delta_{\mathrm{MF}} = 0$, the integral (A.33) reduces to the simple form

$$I_{\pi,0}(z) = N_c \int \frac{\mathrm{d}^3p}{(2\pi)^3}\left[1-n(\xi_{\mathbf{p}}^{+})-n(\xi_{\mathbf{p}}^{-})\right]\frac{2E_{\mathbf{p}}}{z^2-4E_{\mathbf{p}}^2}. \tag{A.34}$$

The function

$$F_{\mathbf{p}}^{\pm}(z) \equiv \frac{1-2n(E_{\mathbf{p}}^{\pm})}{z^2-4\left(E_{\mathbf{p}}^{\pm}\right)^2} \tag{A.35}$$

is the analogue to the function $F(s_p, s_k; t_p, t_k)$ defined above in (A.17) for correlations at rest ($\mathbf{q} = 0$).

### *A.3. Mesonic polarization functions in the normal phase*

In the normal phase the meson and diquark-modes decouple. We denote the mesonic matrix elements by $\Pi_{\pi} \equiv \Pi_{\pi\pi}$, $\Pi_{\sigma} \equiv \Pi_{\sigma\sigma}$. They are explicitly given by the expression

$$\begin{aligned} \Pi_{\pi/\sigma}(z,\mathbf{q}) = & \frac{1}{2}N_f N_c \sum_{s_p,s_k}\int \frac{\mathrm{d}^3p}{(2\pi)^3}\,\mathcal{T}_{-}^{\pm}(s_p,s_k)\frac{n^{-}(s_pE_{\mathbf{p}})-n^{-}(s_kE_{\mathbf{k}})}{z+s_pE_{\mathbf{p}}-s_kE_{\mathbf{k}}} \\ & + (\mu^{*} \to -\mu^{*}), \end{aligned} \tag{A.36}$$

where $\mathcal{T}_{-}^{+}(s_p, s_k)$ holds for the pion case while $\mathcal{T}_{-}^{-}(s_p, s_k)$ for the sigma meson. After analytic continuation to the complex $z$ plane, the analytic properties of the polarization function are captured in its spectral density as defined by the imaginary part of the retarded function, $\mathrm{Im}\,\Pi_{\pi/\sigma}(\omega + \mathrm{i}\eta, \mathbf{q})$.

Results for scalar and pseudo-scalar mesons have already been obtained by *e.g.,* [37,25] and shall be summarized here.

$$\begin{aligned} \mathrm{Im}\,\Pi_{\sigma,\pi}(\omega+\mathrm{i}\eta,\mathbf{q}) = & N_{\pi,\sigma}\frac{N_f N_c}{16\pi|\mathbf{q}|}\{\Theta(s-4m^2)[\Theta(\omega)J_{\mathrm{M,pair}}^{+} \\ & + \Theta(-\omega)J_{\mathrm{M,pair}}^{-}] + \Theta(-s)J_{\mathrm{M,Landau}}\} \end{aligned} \tag{A.37}$$

with

$$J^{\pm}_{\rm M,pair} = T\ln\left[\frac{[1-n^{\pm}(\mathcal{E}^-)]n^{\mp}(\mathcal{E}^-)}{[1-n^{\pm}(\mathcal{E}^+)]n^{\mp}(\mathcal{E}^+)}\right] = T\ln\left[\frac{n^{\mp}(-\mathcal{E}^-)n^{\mp}(\mathcal{E}^-)}{n^{\mp}(-\mathcal{E}^+)n^{\mp}(\mathcal{E}^+)}\right] \tag{A.38}$$

$$J_{\rm M,Landau} = T\ln\left[\frac{n^{+}(\mathcal{E}^-)n^{-}(\mathcal{E}^-)}{n^{+}(-\mathcal{E}^+)n^{-}(-\mathcal{E}^+)}\right] = -2\omega + T\ln\left[\frac{n^{+}(-\mathcal{E}^-)n^{-}(-\mathcal{E}^-)}{n^{+}(\mathcal{E}^+)n^{-}(\mathcal{E}^+)}\right] \tag{A.39}$$

with the Fermi distribution functions $n^{\pm}(E) = [\exp\{(E\pm\mu^*)/T\}+1]^{-1}$ and $\mathcal{E}^{\pm} = \frac{\omega}{2} \pm \frac{|\mathbf{q}|}{2}\sqrt{1-\frac{4m^2}{s}}$.

The kinematic prefactors are $N_\pi = s$ and $N_\sigma = s-4m^2$, with $s = \omega^2 - |\mathbf{q}|^2$. We want to point out, that the imaginary part is an odd function of $\omega$ and consequently the real part is even in $\omega$ so that the spectral function is an odd function of $\omega$.

This form has the thresholds for the occurrence of imaginary parts, given in terms of $\Theta$-functions, explicitly; a property that has been exploited in the discussion of the Mott effect for mesons in Section 4.

### *A.4. Diquark polarization functions in the normal phase*

In the normal phase all diquark modes are degenerate and we denote them as $\Pi_{\rm D} \equiv \Pi_{\delta_A^*\delta_A}$ and $\Pi_{\bar{\rm D}} \equiv \Pi_{\delta_A\delta_A^*}$. The diquark polarization function takes the form

$$\Pi_{\rm D}(z-2\mu^*,\mathbf{q}) = N_f\sum_{s_p,s_k}\int\frac{{\rm d}^3p}{(2\pi)^3}\,\mathcal{T}^+_-(s_p,s_k)\frac{n^+(s_pE_{\mathbf{p}})-n^-(s_kE_{\mathbf{k}})}{z+s_pE_{\mathbf{p}}-s_kE_{\mathbf{k}}}. \tag{A.40}$$

The anti-diquark mode is then obtained by the symmetry relation $\Pi_{\bar{\rm D}} = \Pi_{\rm D}(\mu^*\to-\mu^*)$.

The imaginary part of the retarded diquark polarization function is evaluated to be

$$\mathrm{Im}\,\Pi_{\rm D}(\omega+{\rm i}\eta,\mathbf{q}) = \frac{N_f}{16\pi|\mathbf{q}|}\sum_{a=\pm}s_a\left[\Theta(s_a-4m^2)J^a_{\rm D,pair}+\Theta(-s_a)J^a_{\rm D,Landau}\right] \tag{A.41}$$

with

$$J^{\pm}_{\rm D,pair} = T\ln\left[\frac{1-n^{\mp}(\mathcal{E}^-_{\pm})}{1-n^{\mp}(\mathcal{E}^+_{\pm})}\frac{n^{\mp}(\mathcal{E}^-_{\pm})}{n^{\mp}(\mathcal{E}^+_{\pm})}\right] = T\ln\left[\frac{n^{\pm}(-\mathcal{E}^-_{\pm})}{n^{\pm}(-\mathcal{E}^+_{\pm})}\frac{n^{\mp}(\mathcal{E}^-_{\pm})}{n^{\mp}(\mathcal{E}^+_{\pm})}\right], \tag{A.42}$$

$$J^{\pm}_{\rm D,Landau} = 2T\ln\left[\frac{n^{\mp}(\mathcal{E}^-_{\pm})}{n^{\pm}(-\mathcal{E}^+_{\pm})}\right] = -2\omega + 2T\ln\left[\frac{n^{\pm}(-\mathcal{E}^-_{\pm})}{n^{\mp}(\mathcal{E}^+_{\pm})}\right] \tag{A.43}$$

where we defined $\mathcal{E}^{\pm}_{\mp} = \frac{\omega_{\mp}}{2} \pm \frac{|\mathbf{q}|}{2}\sqrt{1-\frac{4m^2}{s_{\mp}}}$ and $\omega_{\pm} = \omega \pm 2\mu^*$ and $s_{\pm} = \omega_{\pm}^2 - |\mathbf{q}|^2$. Again, the real part of the spectral function is to be evaluated utilizing a Kramers–Kronig relation. This result collapses to the pion imaginary part at $\mu^* = 0$ up to the prefactor 2. For the case of degenerate flavors considered here, the Landau damping term vanishes for correlations at rest ($\mathbf{q} = 0$).

## References


[1] C.D. Roberts, A.G. Williams, Prog. Part. Nucl. Phys. 33 (1994) 477.
[2] P.C. Tandy, Prog. Part. Nucl. Phys. 39 (1997) 117.
[3] R. Alkofer, L. von Smekal, Phys. Rep. 353 (2001) 281.
[4] C.D. Roberts, S.M. Schmidt, Prog. Part. Nucl. Phys. 45 (2000) S1.
[5] H. Kleinert, Phys. Lett. B 62 (1976) 429.
[6] D. Ebert, V.N. Pervushin, in: Tbilisi 1976, Proceedings, Conference on High Energy Physics, Vol. I, Dubna 1976, C125–127.
[7] R.T. Cahill, Aust. J. Phys. 42 (1989) 171.
[8] H. Reinhardt, Phys. Lett. B244 (1990) 316–326.
[9] D. Ebert, H. Reinhardt, M.K. Volkov, Prog. Part. Nucl. Phys. 33 (1994) 1.
[10] R.T. Cahill, J. Praschifka, C. Burden, Aust. J. Phys. 42 (1989) 161.
[11] C.J. Burden, R.T. Cahill, J. Praschifka, Aust. J. Phys. 42 (1989) 147.
[12] J. Praschifka, C.D. Roberts, R.T. Cahill, Phys. Rev. D36 (1987) 209.

[13] U. Zuckert, R. Alkofer, H. Weigel, H. Reinhardt, Phys. Rev. C 55 (1997) 2030.
[14] D. Ebert, H. Reinhardt, Nuclear Phys. B 271 (1986) 188.
[15] C.V. Christov, A. Blotz, H.-C. Kim, P. Pobylitsa, T. Watabe, T. Meissner, E. Ruiz Arriola, K. Goeke, Prog. Part. Nucl. Phys. 37 (1996) 91.
[16] B. Golli, W. Broniowski, G. Ripka, Phys. Lett. B 437 (1998) 24.
[17] R. Alkofer, H. Reinhardt, H. Weigel, Phys. Rep. 265 (1996) 139.
[18] R. Alkofer, H. Reinhardt, Chiral Quark Dynamics, Springer, Berlin, 1995.
[19] G. Ripka, Quarks Bound by Chiral Fields, Clarendon Press, Oxford, 1997.
[20] G.-f. Sun, L. He, P. Zhuang, Phys. Rev. D75 (2007) 096004.
[21] J. Hüfner, S.P. Klevansky, P. Zhuang, H. Voss, Ann. Physics 234 (1994) 225–244.
[22] A. Wergieluk, D. Blaschke, Y.L. Kalinovsky, A. Friesen, Phys. Part. Nucl. Lett. 10 (2013) 660.
[23] K. Yamazaki, T. Matsui, Nuclear Phys. A 913 (2013) 19.
[24] A. Dubinin, D. Blaschke, Y.L. Kalinovsky, Acta Phys. Polon. B Proc. Suppl. 7 (2014) 215.
[25] S. Roessner, T. Hell, C. Ratti, W. Weise, Nuclear Phys. A 814 (2008) 118.
[26] J.-C. Wang, Q. Wang, D.H. Rischke, Phys. Lett. B704 (2011) 347.
[27] W. Bentz, A.W. Thomas, Nuclear Phys. A696 (2001) 138–172.
[28] W. Bentz, T. Horikawa, N. Ishii, A.W. Thomas, Nuclear Phys. A720 (2003) 95.
[29] S. Lawley, W. Bentz, A.W. Thomas, J. Phys. G G32 (2006) 667.
[30] A. Bazavov, et al., Phys. Rev. D 85 (2012) 054503.
[31] S. Borsanyi, et al., [Wuppertal-Budapest Collaboration], J. High Energy Phys. 1009 (2010) 073.
[32] K. Fukushima, Phys. Lett. B 591 (2004) 277.
[33] E. Megias, E. Ruiz Arriola, L.L. Salcedo, Phys. Rev. D 74 (2006) 065005.
[34] C. Ratti, M.A. Thaler, W. Weise, Phys. Rev. D 73 (2006) 014019.
[35] H. Hansen, W.M. Alberico, A. Beraudo, A. Molinari, M. Nardi, C. Ratti, Phys. Rev. D 75 (2007) 065004.
[36] S.P. Klevansky, Rev. Modern Phys. 64 (1992) 649.
[37] T. Hatsuda, T. Kunihiro, Phys. Rep. 247 (1994) 221.
[38] M. Buballa, Phys. Rep. 407 (2005) 205.
[39] U. Vogl, W. Weise, Prog. Part. Nucl. Phys. 27 (1991) 195.
[40] T. Klähn, D. Blaschke, F. Sandin, C. Fuchs, A. Faessler, H. Grigorian, G. Röpke, J. Trümper, Phys. Lett. B 654 (2007) 170.
[41] J.I. Kapusta, Finite Temperature Field Theory, Cambridge University Press, Cambridge, 1989.
[42] D. Ebert, K.G. Klimenko, V.L. Yudichev, Phys. Rev. C 72 (2005) 015201.
[43] D. Blaschke, D. Ebert, K.G. Klimenko, M.K. Volkov, V.L. Yudichev, Phys. Rev. D 70 (2004) 014006.
[44] H.B. Nielsen, S. Chadha, Nuclear Phys. B 105 (1976) 445.
[45] T. Brauner, Phys. Rev. D 75 (2007) 105014.
[46] H. Watanabe, T. Brauner, Phys. Rev. D 84 (2011) 125013.
[47] D.D. Dietrich, D.H. Rischke, Prog. Part. Nucl. Phys. 53 (2004) 305.
[48] D.S. Zablocki, D. Blaschke, M. Buballa, Phys. Atomic Nuclei 75 (2012) 910.
[49] N. Strodthoff, B.-J. Schaefer, L. von Smekal, Phys. Rev. D 85 (2012) 074007.
[50] V. Kleinhaus, M. Buballa, D. Nickel, M. Oertel, Phys. Rev. D 76 (2007) 074024.
[51] G. Uhlenbeck, E. Beth, Physica 3 (1936) 729.
[52] E. Beth, G. Uhlenbeck, Physica 4 (1937) 915.
[53] R. Zimmermann, H. Stolz, Phys. Status Solidi (b) 131 (1985) 151.
[54] W.D. Kraeft, D. Kremp, W. Ebeling, G. Röpke, Quantum Statistics of Charged Particle Systems, Plenum, New York, Akademie-Verlag, Berlin, 1986.
[55] G. Röpke, L. Münchow, H. Schulz, Nuclear Phys. A 379 (1982) 536.
[56] N. Levinson, D. Kgl. Danske Vidensk. Selskab. Mat.-fys. Medd. XXXV (9) (1949).
[57] R. Dashen, S.-K. Ma, H.J. Bernstein, Phys. Rev. 187 (1969) 345.
[58] M. Schmidt, G. Röpke, H. Schulz, Ann. Physics 202 (1990) 57.
[59] H. Abuki, Nuclear Phys. A791 (2007) 117.
[60] P. Zhuang, J. Hüfner, S.P. Klevansky, Nuclear Phys. A 576 (1994) 525.
[61] G. Röpke, N.-U. Bastian, D. Blaschke, T. Klähn, S. Typel, H.H. Wolter, Nuclear Phys. A 897 (2013) 70.